TESLA - COLLABORATION

PAC 93 Contributions

May 17 - 20, 1993
Washington, D.C.

DESY Print August 1993, TESLA 93-33

TESLA-Collaboration - PAC 93 Contributions

Table of Contents

Presented as Poster Sa44 at the 1993 Particle Accelerator Conference, Washington DC, May 1993. CLNS 93/1217

A World Record Accelerating Gradient in a Niobium Superconducting Accelerator Cavity*

J. Graber‡, P. Barnes, J. Kirchgessner, D. Moffat, H. Padamsee, and J. Sears
F.R. Newman Laboratory of Nuclear Studies
Cornell University
Ithaca, NY 14853 USA

Abstract

A two-cell, 3 GHz, niobium superconducting accelerator cavity has sustained a continuous wave (CW) accelerating gradient of 34.6 MV/m, with corresponding peak surface electric electric field of 100 MV/m, record performances in each category for a superconducting accelerator cavity. Field emission (FE) loading of the cavity initially limited the cavity to E_{acc} = 21 MV/m (E_{peak} = 60 MV/m). The record field was achieved by reducing the FE loading through High Peak Power (HPP) RF processing of the cavity. Analysis of previous results of the HPP experimental program indicated that maximum fields under both pulsed and CW conditions were limited by thermal breakddown, which is related to the surface magnetic field in the cavity. The two-cell cavity shape was chosen to bypass the thermal breakdown limitations by reducing the ratio of peak surface magnetic field to peak surface electric field, from a value of H_{peak}/E_{peak} = 23 Oe/(MV/m) in the previous cavity, to 14 Oe/(MV/m) in the two-cell cavity. A simple thermal model accurately simulates the pulsed breakdown.

I. INTRODUCTION

A. SRF Cavities

Niobium Superconducting Radio-frequency (SRF) cavities are a promising technology for construction of the next generation of electron-positron colliders. In order for SRF to become a viable method for construction of these machines, however, attainable accelerating gradients must be increased from the 5-10 MV/m attained in present SRF accelerators to 25-30 MV/m.[1] The gradients reached in this work show that it is possible to achieve the desired performance for TeV colliders, using HPP to overcome field emission (FE), the major limitation to high gradients.

The HPP experiment was designed to explore the benefits of high power pulsed radio-frequency (RF) processing as a means of reducing FE loading in 3 GHz niobium accelerator cavities. RF processing is a method of cavity conditioning, where the cavity is exposed to high RF fields in the absence of a particle beam. The HPP apparatus can deliver up to 200 kW peak power for millisecond pulse lengths during processing. An in depth description of all results of the HPP experiments can be found in the Ph.D. dissertation associated with this work.[2]

B. Thermal Limitations of Previous HPP Work

The HPP experiments have shown that high power processing is a successful method of reducing FE loading in SRF cavities.[3] The initial studies were performed with single-cell and nine-cell cavities, using a geometry termed the S3C geometry. Results of the tests on nine-cell cavities are being presented in another paper to be presented at this conference.[4] Success in FE reduction via processing has been directly linked to the magnitude of the electric field attained during processing (E_{HPP}). Furthermore, the attainable E_{HPP} has been shown to be limited by thermal breakdown, the phenomena where the RF surface is locally heated above the critical temperature, initiating the growth of a normal conducting region. Thermal breakdown limited single-cell cavities to E_{peak} = 55 MV/m (H_{peak} = 1265 Oe) CW and E_{peak} = 72 MV/m (H_{peak} = 1650 Oe) during HPP. Nine-cell cavities reached E_{peak} = 42 MV/m (H_{peak} = 840 Oe) CW and E_{peak} = 62 MV/m (H_{peak} = 1250 Oe) during HPP.

Thermal breakdown is driven by the surface currents which are required to support the magnetic fields at the RF surface. We therefore chose to investigate a cavity with a lower ratio of H_{peak}/E_{peak}. This ratio is determined by the cavity geometry, and can be obtained by numerical solution of Maxwell's Equations. Several programs exist for this purpose, e.g. SUPERFISH[5]. The S3C cavities used for the single-cell and nine-cell experiments have H_{peak}/E_{peak} ratios of 23 Oe/(MV/m) and 20 Oe/(MV/m), respectively.

II. TWO-CELL W3C2-1

A. Cavity Fabrication and Preparation

After some investigation of potential cavity shapes, we chose a two-cell cavity using the geometry of the SRF group at the University of Wuppertal. A larger rounding of the equator region reduces the magnetic to electric field ratio of this cavity, designated W3C2-1, to H_{peak}/E_{peak} = 14.2 Oe/(MV/m). Interatom GmbH graciously agreed to press the half cells for this cavity (gratis). Final trimming, yttrification (for purification, and thus higher thermal conductivity), and electron beam welding were performed at Cornell.

The initial attempts at testing this cavity were limited by anomolously low thermal breakdown, initially due to insufficient surface chemistry then later due to the "Q virus." The final preparation prior to the successful test was a 2 hour bake at 900° C to eliminate the hydrogen contamination which has been identified as the cause of the Q virus.

B. Cold RF Measurement

Based on the reduced H_{peak}/E_{peak} ratio and the observed magnetic field break-down levels (H_{bd} = 1250-1300 Oe) from the S3C cavities, we predicted that the cavity would reach 90-95 MV/m prior to thermal breakdown limitation. The cavity performance exceeded this prediction. The results of the best experiment with cavity W3C2-1 are shown in Figure 1. This cavity experiment extended over two cool downs, with a room temperature cycle, but no vacuum break between.

* Supported by the NSF with supplementary support from the U.S.-Japan Collaboration.

‡ Permanent Address: DESY, 85 Notkestrasse, 2000 Hamburg 52, Germany.

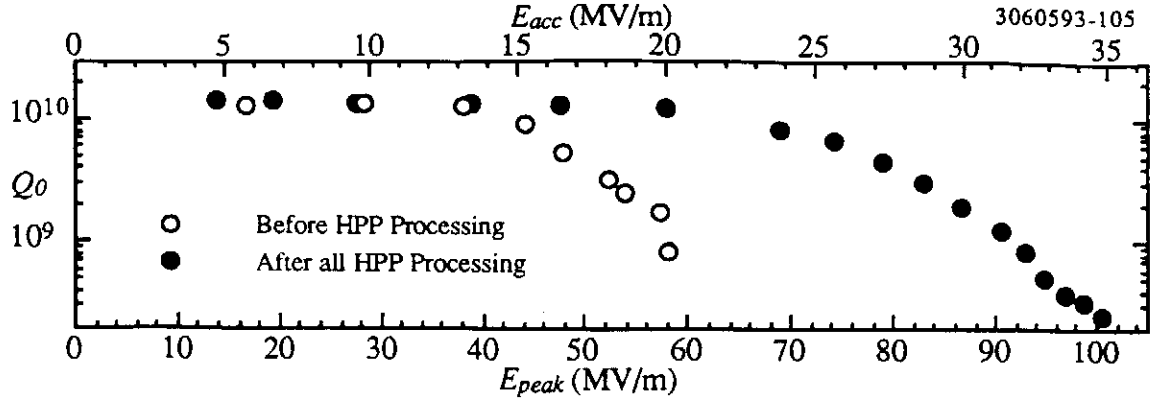

Figure 1. Q_0 vs. E_{peak} (E_{acc}) plots for the best experiment with cavity W3C2-1.

On initial rise of power, the cavity performance was simi- was measurable at E_{peak} = 25 MV/m, though low power processing with P_{inc} = 10 W increased the threshold to E_{peak} = 35 MV/m. The second plot in Figure 1 is the best CW measurement from the second day of testing the cavity. This CW measurement followed processing with incident power up to 130 kW, and fields as high as E_{HPP} = 103 MV/m, a room temperature cycling, and processing with power up to 100 kW, and fields as high as E_{HPP} = 113 MV/m. During HPP, analysis indicates that Q_0 values dropped to 10^6. As can be seen, the improvement is remarkable. The maximum attained CW field was E_{peak} = 100.6 MV/m, limited by thermal breakdown (H_{peak} = 1430 Oe). This peak electric field is 20 MV/m higher than any accelerating cavity has ever been operated CW. The corresponding accelerating gradient at E_{peak} = 100.6 MV/m was E_{acc} = 34.8 MV/m. The Q_0 of the cavity remained above 5 x 10^9 for peak fields as high as 75 MV/m (E_{acc} = 26 MV/m). The experiment was repeated, reaching E_{peak} = 85 MV/m (with nearly identical field emission behavior), where it was limited by a superfluid helium leak.

C. Comparison with Previous HPP Results

We can now compare the results of all tests of two-cell cavity W3C2-1 with the results of tests of the S3C shape cavlar to that of pre-HPP single cell cavities. FE related Q_0 drop ities. Figure 2 plots maximum attainable CW electric field as a function of the maximum processing field preceding the CW measurement. The results of the two cell cavity are in good agreement with an extrapolation of the single-cell and nine-cell results. Furthermore, this clearly supports the correlation between processing field and success in processing.

Figure 3 is a similar plot, showing the X-ray detection threshold electric field as a function of maximum E_{HPP}. X-rays are produced when emitted electrons impact elsewhere in the cavity, and X-ray detection is a reproducible method of characterizing the onset of field emission in a cavity.

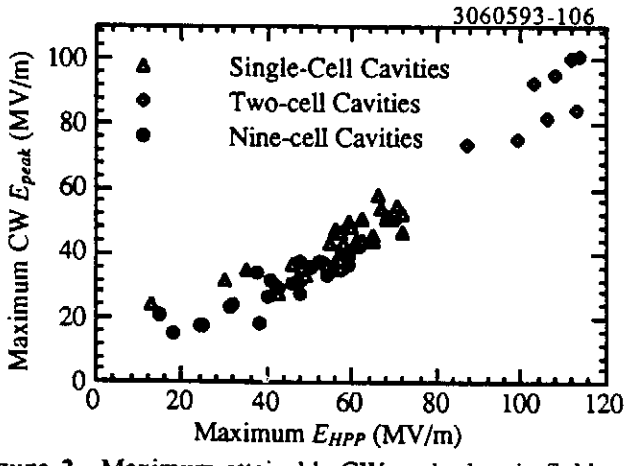

Figure 2. Maximum attainable CW peak electric field as a function of peak field attained during HPP processing. Note that the two-cell cavity behavior is in good agreement with an extrapolation of nine-cell and single-cell behavior.

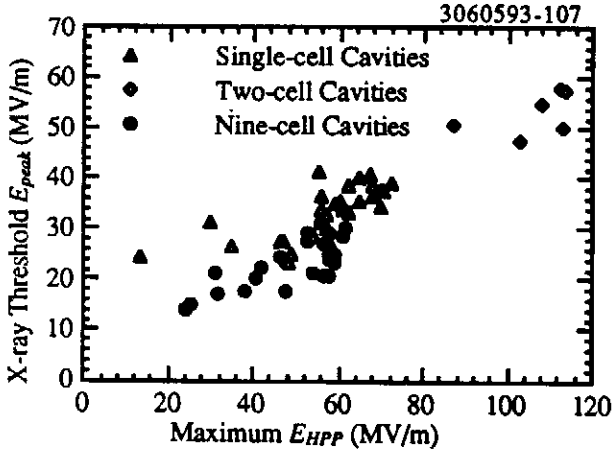

Figure 3. X-ray threshold peak electric field as a function of peak field attained during HPP processing.

III. MODELING OF THERMAL LIMITATIONS

A. The Model

With the predominance of thermal breakdown as a limitation to attainable fields during processing (and therefore success in processing), it is instructive to model the thermal processes in the cavity. Previous work on modeling (e.g. program **HEAT**[6]) has been done on the simplified system of a niobium disk, with magnetic fields (power input through dissipation) at one circular face, and a helium bath (cooling) at the opposite face. Steady state solutions of this problem provided reasonable predictions for thermal breakdown field levels

in typical cavities. More recently, this model was expanded, in program **Transient_HEAT**,[7] to include transient effects. With **Transient_HEAT**, we were able to gain an initial understanding of the time evolution of a normal conducting region on a superconducting surface. With this understanding, the following model was developed.

We allow for four different loss mechanisms: superconducting wall losses, FE losses, input coupler losses, and normal conducting wall losses. FE losses are estimated by extrapolating the low field behavior to HPP conditions.

We assume the cavity has a single breakdown initiation region, which activates at a fixed magnetic field (H_{BD}). When H_{BD} is surpassed, a circular normal conducting region begins to grow on the RF surface of the cavity, with expansion velocity v_{nc}, which was obtained by determining the growth rate of the normal conducting region as a function of magnetic field with **Transient_HEAT**. The results of **Transient_HEAT** indicate that v_{nc} varies quadratically with increasing magnetic field, with a typical growth rate being 500 m/s for RRR = 400, H_{BD} = 1200 G, $H_{surface}$ = 1400 G.

During application of high pulsed power, it is possible to exceed the CW thermal breakdown field while the NC region grows in size. The amount of overshoot is a function of many parameters, including incident power, CW breakdown field, loaded Q, FE loading.

A more complete description of this model can be found in the previously mentioned dissertation.[2]

B. Model Predictions and Analysis

The result of simulation is an explaination of the relationship between CW thermal breakdown field and the attainable peak field during HPP. Given the experimental conditions of RF processing, this model predicts the "overshoot" of CW breakdown field. Figure 4 is a comparison of measured and predicted E_{HPP}, as only the input coupling (designated by Q_{ext}) changes; pulse length and input power remain constant. The CW thermal breakdown field and the predicted peak field without taking breakdown into account are also shown for reference.

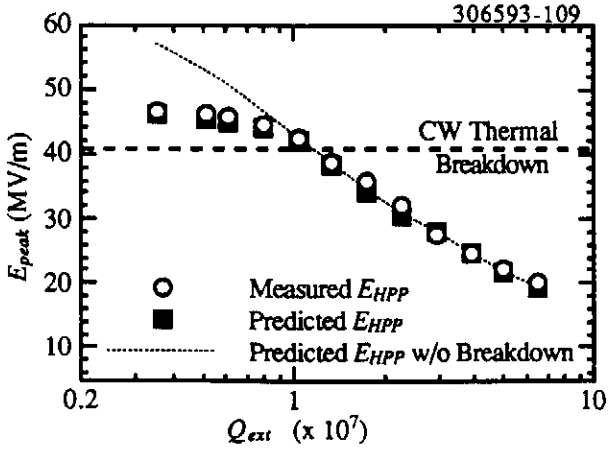

Figure 4. Comparison of Measured and Predicted E_{HPP} during HPP on a nine-cell cavity.

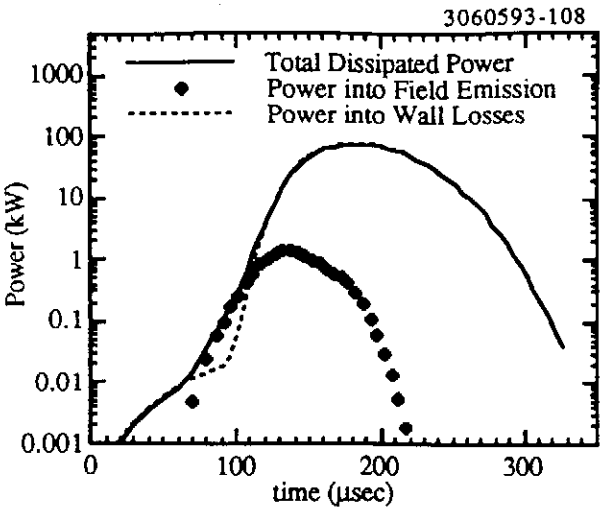

Figure 5. Power dissipation as a function of time during pulsed operation of a nine-cell cavity in quench conditions. Note that FE losses account for only 1% of total dissipation.

With this model, we are also able to analyze where the power being dissipating during HPP processing. HPP was performed with 50 kW (maximum) on single-cell cavities, 130 kW on the two-cell cavity, and 200 kW on nine-cell cavities. Based on this analysis, however, we find that if thermal breakdown is occurring during the HPP, a very small part of the dissipated power is going into field emission. Figure 5 shows an example of the time evolution of the power dissipation in a nine-cell cavity with 200 kW peak power incident upon it. While the power dissipation reached as high as 100 kW, we find that only slightly more than 1 kW was coupled into FE. Similarly, we find that in all single-cell, two-cell, and nine-cell tests, if thermal breakdown is occurring, then FE losses account for no more than 5% of the total losses. In order to optimize future HPP processing, thermal breakdown must be avoided if possible. Possible methods include higher purity material, lower RF frequencies, or lower H_{peak}/E_{peak} ratios. The last method was successfully implemented in cavity W3C2-1, allowing the record performance reported here.

IV. ACKNOWLEDGMENTS

We wish to thank G. Mueller at Wuppertal, and M. Peiniger and D. Dasbach at Interatom for their assistance in fabrication of the W3C2-1 cavity.

V. REFERENCES

[1] *Proc. of the 1st TESLA Workshop*, Cornell University, Ithaca, NY, CLNS **90-1029** (1990).
[2] J. Graber, Ph.D. Dissertation, Cornell University (1993).
[3] J. Graber, et al., *Proc. of the 5th Workshop on RF Superconductivity*, D.Proch ed., DESY, Hamburg, Germany, **DESY M-92-01**, 576 (1992).
[4] J. Graber, et al., this conference, poster Sa42.
[5] K. Halbach and R.F. Holsinger, *Part. Acc.* 7, 213 (1976).
[6] H. Padamsee, **CERN/EF/RF 82-5** (1982).
[7] X. Cao, ibid. ref. 3, 727 (1992).

CLNS 93/1211

Presented at the 1993 Particle Accelerator Conference, May 17-20, 1993 Washington, D.C.

20 MV/m Accelerating Gradient with Heat Treatment of a Six Cell, 1.5 GHz Cavity for TESLA,*

J. KIRCHGESSNER, P. BARNES, W. HARTUNG, M. HILLER†, D. MOFFAT, H. PADAMSEE, D. RUBIN, D. SARANITI††, J. SEARS, Q. S. SHU†††, and M. TIGNER
Laboratory of Nuclear Studies, Cornell University, Ithaca, NY 14853 USA

SUMMARY

In order to use superconducting RF accelerating structures in the construction of a high energy linear collider, the structures must be designed to meet specific goals. These include low peak surface electric fields, good higher order mode power extraction from the ends, maximum accelerating gradient and, above all, low cost per unit accelerating voltage. Such a structure has been designed, manufactured and tested. Preliminary results have been reported.[1] The cavity was then mechanically braced with Niobium braces and then heat treated. The final test gave 20 MV/m accelerating field. Details of some difficulties encountered will also be presented at this time.

INTRODUCTION

At this time in the development of superconducting RF accelerating cavities, the accelerating gradient is limited by two phenomena, electron field emission and thermal breakdown. The first of these makes it imperative to choose a cell shape that minimizes E_{pk}/E_{acc} and the second phenomena to minimize H_{pk}/E_{acc} (the ratio of the peak surface fields to the accelerating gradient). As field emission is the dominant gradient limitation, there is considerable premium in lowering E_{pk}/E_{acc}. The cell to cell coupling (K) is also effected by the shape. This is true of the coupling of the HOM's as well as the fundamental TM_{010} mode. Because of this, the number of coupled cells comprising an accelerating unit is limited. A larger number of cells/module helps reduce the structure cost by reducing the number of couplers as well as by improving the filling factor for the machine. Another consequence of the cell to cell coupling in the TM_{010} mode is the relative ease of tuning the structure to achieve uniform accelerating gradient along the length of the unit.

DESIGN OF THE STRUCTURE

In order to test our ability to produce an accelerating structure which best meets the requirements of a linear collider, a series of calculations were made in which we tried to design the shape of the structure which had the following properties:

- Low E_{pk}/E_{acc}.
- Tolerable cell to cell coupling (K) in the TM_{010} mode.
- More than 5 cells/unit.
- Low cost.
- Tolerable Q_{ext} in all HOM's with couplers on the beam pipe.

Although it is straightforward to reduce E_{pk}/E_{acc} by reducing the beam pipe radius BT, this is undesirable because the transverse wakefields increase as BT^{-3} which makes it more difficult to control multibunch instabilities and meet alignment and vibration tolerances for the linac.

The cavity shape that was manufactured and tested is shown in Figure 1.

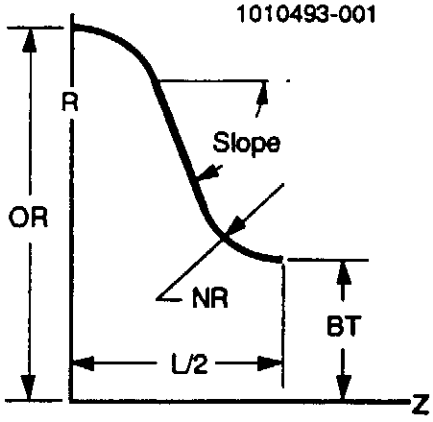

Figure 1.

The five independent variables describing the shape were as follows:

OR, the outside radius.
BT, the beam tube radius.
L/2, the half length of the cell.
NR, the nose radius, and
Slope, the slope of the straight wall segment.

The OR which primarily determines the fundamental mode frequency is adjusted in all cases to obtain the desired frequency. The L/2 value is determined by the frequency as the particles to be accelerated must be kept in phase with the RF oscillations. Namely L/2 must be equal to 1/4 wavelength.

In order to minimize the number of couplers required on the cavity module, the cells were polarized in a manner such that both polarizations of the dipole modes could be damped with one coupler.[2]

CONSTRUCTION

The cavity chosen to best meet the stated requirements was manufactured of 1.5 mm Niobium sheet and was 6 cells long. The number of 6 cells was limited by the available furnace and by the available testing facilities. The cell parameters are shown in Table 1.

---

* Supported by the National Science Foundation, with supplementary support under the U. S. -Japan Agreement.
† Babcock & Wilcox, Lynchburg, VA
†† Now at Stanford University, Palo Alto, CA

††† Now at SSC Laboratory

Frequency	1500 MHz
OR(Equator Radius)(average)	9.48 (9.43 ends) cm
NR(Nose Radius)	1.09 cm
BT(Beam Tube Radius)	3.56 cm
Slope	70 degrees
L/2(1/2 cell length)	4.93 cm
Coupling K	1.8%
E_{pk}/E_{acc}	2.1
R/Q	89 ohms /cell
H_{pk}/E_{acc}	57 gauss/MV/meter
Length of Polarizing Segment	1.27 cm
% Freq. Split of TM_{110} mode	2.9% (2.03 GHz)
% Freq. Split of TE_{111} mode	0.22% (2.02 GHz)

Table 1

TESTS OF CAVITY

This six cell niobium cavity (LTP6-1) was initially tested twice. In both tests the structure reached fields of E_{acc}=18 MV/meter with considerable field emission, but final thermal breakdown. These tests were reported in Reference 1 and the curves from these tests are shown in Figure 2.

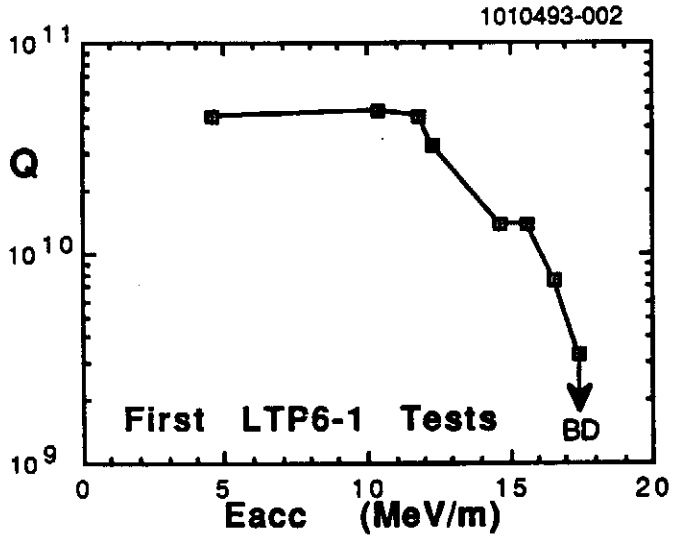

Figure 2

In order to reduce field emission we wished to vacuum fire the structure. Because the cell walls were only 1/16" thick, thr. : longitudinal braces were welded to the equator of each of the cells to prevent distortion during firing and collapse during later tests.

In the process of welding on these braces, a gun arc in the EBW (electron beam welder) melted a 1/2" diameter hole in one of the cells. A very careful repair was made and when the cavity was remeasured at room temperature it was found to still retain adequate tune of all cells to give a level field profile.

The cavity was retested at this stage and the results were not very good. There was thermal breakdown at an E_{acc} level of 8-10 MV/meter. This data is shown in Figure 3.

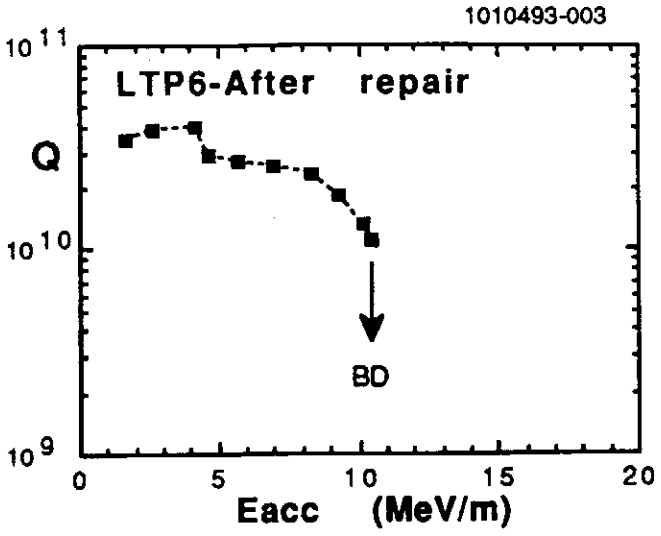

Figure 3

After a heavy etch to hopefully remove the apparent new defect, the cavity was fired for four hours at 1500 deg. C in a standard titanium lined niobium box.[3] After firing, the structure was rinsed, but the titanium was not chemically removed from the outside of the structure. In this test, the E_{acc} value achieved was 15.3 MV/meter. The results of this test is shown in Figure 4.

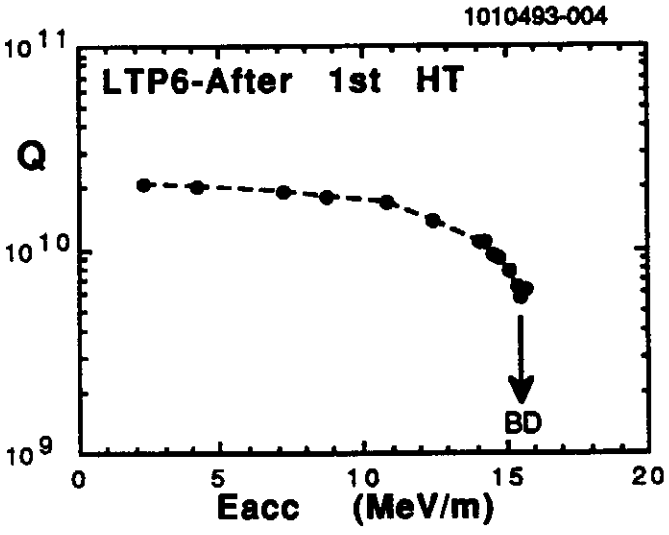

Figure 4

After this test the field flatness was measured to see if the firing had detuned the cavity. The E_{max}/E_{min} cell ratio was measured to be 1.9. This value of cell to cell field variation is excessive. During the firing the braced cavity was suspended from the top beam tube. This caused the top end half cell to be deformed by the force applied to it while the niobium was in the hot, softened condition. It was found that by tuning only

the top half cell, that had taken all the cavity weight, the cell fields could be completely leveled.

After this first heat treating, the field level in the cavity was still not quite as high as the field achieved in the first tests. In an attempt to push to higher fields, the cavity was again chemically etched and fired for 4 more hours at 1500 C. After firing, the cavity was tuned in the clean room. This was followed by a Methanol rinse followed by ultrasonic cleaning with Methanol, then a final Methanol rinse.

After mounting, the cavity was again tested and the results are shown in Figure 5.

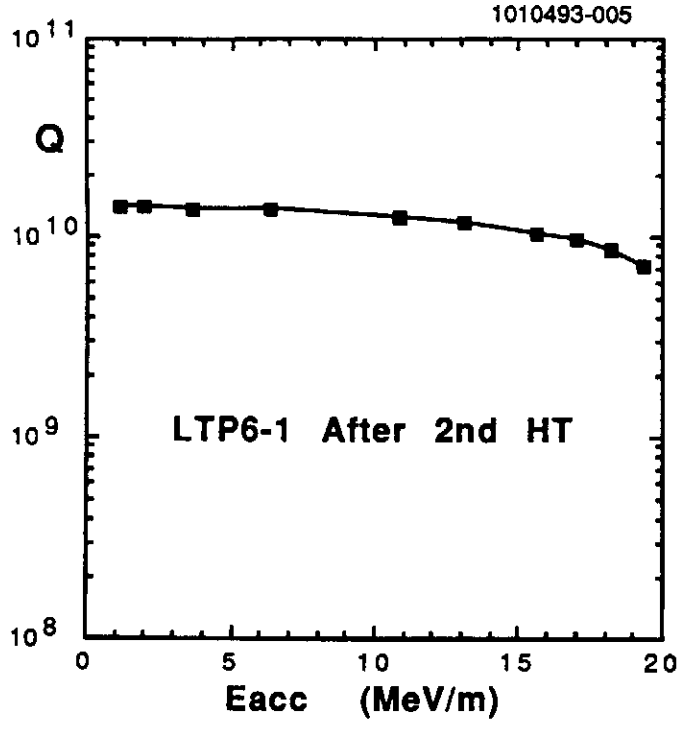

Figure 5

As can be seen, the field level of E_{acc}= 19.5 MV/m at a very good Q value was finally realized.

CONCLUSIONS

Several important lessons were learned in the course of the experiments on this cavity structure. They could be listed as follows:

- The ratio of H_{pk}/E_{acc} must be watched when the cell shape is designed. Since the time when this cavity shape was developed a new shape has been developed for TESLA which does not suffer from this high value of H_{pk}/E_{acc}.
- Sometimes a very good result is achieved on the first test.
- Bracing of the cells is very effective in stabilizing the parts that are braced.
- Furnace treatment with Titanium is effective in increasing RRR and, therefore, raising the thermal breakdown limits.
- Very extensive repairs may be made on the cells with no long term bad effects.
- Chemical cleaning of the structure seems to completely restart history in terms of the surface field emission behavior.
- Polarized cells seem to exhibit no different behavior in the TM_{010} mode by virtue of being polarized.
- Careful records were kept of the costs of the manufacture and treatment of this structure. The total was less than $6000.
- Bead pull measurements can be made on a cavity in a clean room, under clean conditions without introducing excessive field emitters that are difficult to remove.

The experiments with this structure were important steps in the process of achieving high field, low cost superconducting linear collider cavities.

REFERENCES

[1] J. Kirchgessner et. al., Proc. 1991PAC, San Francisco, p 2426
[2] J. Kirchgessner et. al., Proc. 1989 PAC, Chicago, p 479
[3] Q. S. Shu et. al., Proc. 1989 PAC, Chicago, p 491

Presented as Poster Sa42 at the 1993 Particle Accelerator Conference, Washington DC, May 1993. CLNS 93/1215

An Update on High Peak Power (HPP) RF Processing of 3 GHz Nine-cell Niobium Accelerator Cavities*

J. Graber‡, P. Barnes, C. Crawford†, J. Kirchgessner, D. Moffat, H. Padamsee, P. Schmüser‡, and J. Sears
F.R. Newman Laboratory of Nuclear Studies
Cornell University
Ithaca, NY 14853 USA

Abstract

Two 3 GHz, nine-cell niobium accelerator structures have been fabricated and tested multiple times. An unambiguous improvement in cavity performance can be shown due to High Peak Power (HPP) RF processing of the cavities. The average achieved accelerating gradient prior to HPP processing was E_{acc} = 12 MV/m, (Standard Deviation = 3 MV/m). The average maximum accelerating gradient following all HPP processing was E_{acc} = 17 MV/m, (Standard Deviation = 2 MV/m). Gains in cavity performance can be directly correlated with magnitude of field reached during pulsed HPP processing. Durability of processing gains has been tested by exposing processed cavities to filtered air, at room temperature, and unfiltered air, under both room temperature and cryogenic conditions. Filtered air had no discernable effect on cavity performance. Unfiltered air degraded cavity performance, through increased emission, however much of the cavity performance could be regained through further RF processing.

I. INTRODUCTION

Superconducting Radio-frequency (SRF) cavities are a promising technology for construction of the next generation of electron-positron colliders. In order for SRF to become a viable method for construction of these machines, however, attainable accelerating gradients must be increased from the 5-10 MV/m attained in present SRF accelerators to 25-30 MV/m.[1] Field emission (FE) of electrons from the RF surface has been the primary limitaion to SRF cavities for the last five to ten years.

The HPP experiment was designed to explore the benefits of high power pulsed radio-frequency (RF) processing as a means of reducing FE loading in 3 GHz niobium accelerator cavities. RF processing is a method of cavity conditioning, where the cavity is exposed to high RF fields in the absence of a particle beam. The HPP apparatus can deliver up to 200 kW peak power for millisecond pulse lengths during processing.

Early results with HPP (presented previously[2],[3]) showed significant reduction in FE loading in single-cell cavities. It is also important to verify that the HPP technique can successfully reduce FE loading in multi-cell structures as well as it does in single cavities. Two nine-cell cavities were constructed and tested several times each. Between successive tests on a cavity, an acid etch was performed, removing approximately 10 microns from the RF surface. Past studies lead us to believe that retesting following etching is equivalent to testing a new cavity. A complete description of the HPP experiments can be found in the Ph.D. dissertation associated with this work.[4]

II. OVERVIEW OF NINE-CELL RESULTS

In this paper, we will show that HPP is successful in improvement of low power, continuous wave (CW) behavior of the nine-cell cavities. To support this conclusion, we report on investigation of cavity performance before and after HPP processing, as well as correlation of the improvements with the characteristics of HPP processing.

Figure 1 is a histogram comparison of attainable CW accelerating gradient, before and after HPP processing. HPP processing improved the mean attainable gradient from 12 MV/m to 17 MV/m, an increase of 41%.

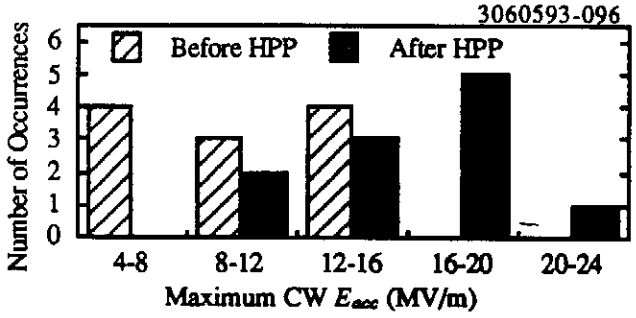

Figure 1. Histogram plot of maximum achieved CW accelerating gradient, before and after HPP processing. Without HPP, $\langle E_{acc} \rangle$ = 11.9 MV/m (s.d. = 3.4 MV/m). With HPP, $\langle E_{acc} \rangle$ = 17.0 MV/m (s.d. = 2.1 MV/m).

Figure 2 is a histogram comparison of X-ray detection threshold gradient, before and after HPP processing. X-rays are produced when emitted electrons impact elsewhere on the cavity surface. The onset of X-rays is a reproducible method of detecting the onset of FE. HPP processing improved the

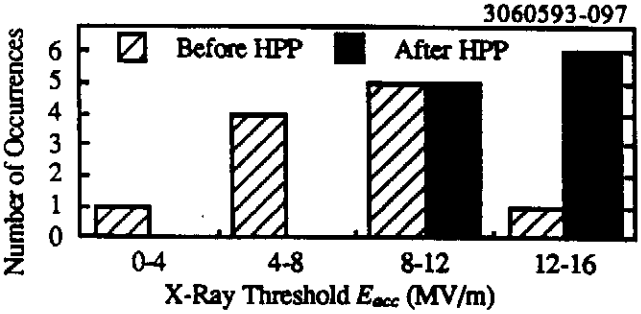

Figure 2. Histogram plot of X-ray threshold accelerating gradient, before and after HPP processing. Without HPP, $\langle E_{acc} \rangle$ = 7.5 MV/m (s.d. = 1.3 MV/m). With HPP, $\langle E_{acc} \rangle$ = 12.4 MV/m (s.d. = 1.3 MV/m).

Supported by the NSF with supplementary support from the U.S.-Japan collaboration.

† Permanent Address: Fermilab, Batavia, IL USA.

‡ Permanent Address: DESY, 85 Notkestrasse, 2000 Hamburg 52, Germany.

X-ray threshold gradient from 7.5 MV/m to 12.4 MV/m, an increase of 65%.

Figure 3 shows a composite plot of the Q_0 vs E_{acc} plots of the best six experiments with nine-cell cavities. When the FE threshold is exceeded in a cavity, the dissipated power grows exponentially with increasing electric fields, causing the severe drop in Q_0, as shown in Figure 3.

III. ANALYSIS

Given the success in improving CW behavior of the nine-cell cavities, we would like to characterize the success with relation to the terms of the HPP parameters. A clear correlation can be shown between the electric field reached during HPP processing (E_{HPP}) and the subsequent CW cavity performance. Figure 4 is a plot of maximum attained field as a function of

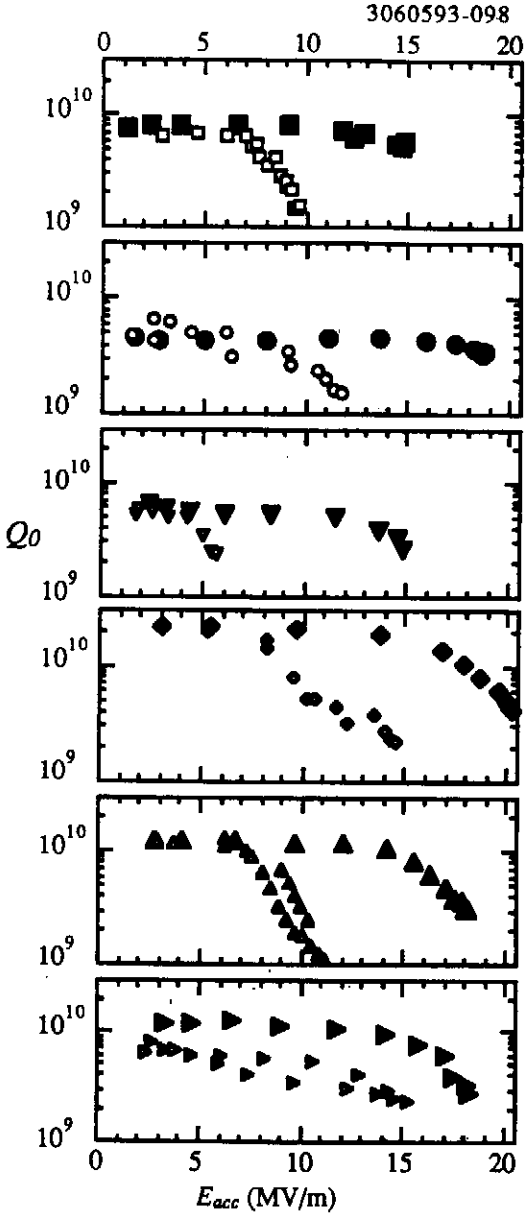

Figure 3. Composite Q_0 vs E_{acc} plots of the six best tests of nine cell cavities. Open symbols show cavity behavior before processing; closed symbols are for after HPP.

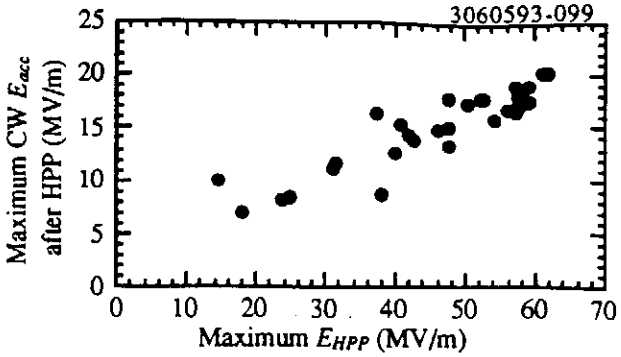

Figure 4. Maximum attained CW E_{acc} plotted as a function of maximum surface electric field during HPP processing.

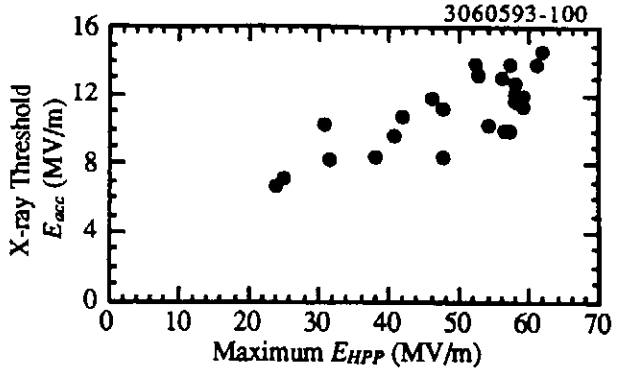

Figure 5. CW FE loading threshold E_{acc} plotted as a function of maximum surface electric field during HPP processing.

E_{HPP}. Figure 5 is a plot of X-ray threshold as a function of E_{HPP}. In these plots we see that increasing E_{HPP} generally leads to reduced FE, and therefore increased attainable accelerating gradients. During HPP, the input power, loaded Q, and pulse length are adjusted to maximize E_{HPP}. We additionally found that in any individual experiment, when E_{HPP} stopped improving, no further reduction of FE was achieved. Q_0 values are estimated to drop as low as 10^6 during HPP.

The current working model for RF processing states that processing occurs when the electric fields are driven sufficiently high so as to induce an emission current which is strong enough to cause melting and/or vaporization of the emission site. This model is supported by the correlation of processing success with E_{HPP}. The microscopic effects of RF processing are more fully investigated in another paper presented at this conference.[5]

The primary limitation on E_{HPP} has been determined to be thermal breakdown (or quench), where the RF surface of the cavity is locally heated above the critical temperature. It then becomes normal conducting. Methods of characterizing and overcoming the quench limit are further discussed in another paper presented at this conference.[6]

IV. OTHER RESULTS

A. *Durability of Processed Cavities*

HPP processing is foreseen as a possible method of cavity preparation for large scale accelerator facilities. In order to show the applicability to this function, it is necessary to learn what care is required for a cavity following processing to

maintain the HPP induced benefits. To this end, we allowed a processed nine cell cavity (low field $Q_0 = 1 \times 10^{10}$, $Q_0 > 10^{10}$ for E_{acc} = 14 MV/m, maximum E_{acc} = 18 MV/m) and cycled it to room temperature. While at room temperature, the cavity was exposed to filtered air (0.3 micron HEPA filter) for 24 hours, and then re-evacuated. The cavity was then re-cooled to liquid helium temperature, and the FE behavior was measured. Figure 6 shows the Q_0 vs. E_{acc} plots before and after this exposure. No significant change in FE loading is seen.

This is consistent with the findings of RF processing studies performed on low frequency, heavy ion accelerator cavities at Argonne National Laboratory[7], as well as low power processing of 1.5 GHz cavities at Cornell LNS.[8]

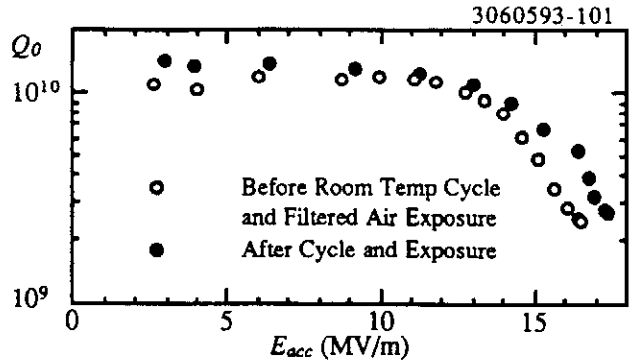

Figure 6. Q_0 vs. E_{acc} plots showing nine-cell cavity behavior before and after a room temperature cycle, with exposure to filtered air. No significant change in FE behavior is measured.

B. Recovery from Vacuum Accidents

Vacuum accidents are an ever present danger in accelerator systems, and the contamination due to such an accident can cause significant degradation of the performance of an accelerator cavity. In this light, we present the results of two exposures of nine cell cavities to unfiltered air, one accidental and one intentional.[9] It has been established previously that air, especially unfiltered air, is a source of field emitters.[8],[10]

The circumstances of the first accident were: At T = 4.2 K, the cavity was exposed to the vacuum pumps which are used to evacuate the experimental dewar in order to reduce the temperature to 1.4 K. Following re-evacuation of the cavity, the experiment was begun. The Q_0 vs. E_{acc} plots are shown in Figure 7. The initial rise of power was characterized by very heavy FE, some of which was processable with low power. The second curve in Figure 7 is the reproducible Q_0 vs. E_{acc}, following all possible low power processing. The cavity was then HPP processed with power as high as 90 kW, and fields as high as E_{peak} = 58 MV/m. The HPP processing was not only successful in reducing the FE loading, but it also seemingly improved the low field Q_0 value, possibly through RF removal of resistive contaminants on the cavity surface.

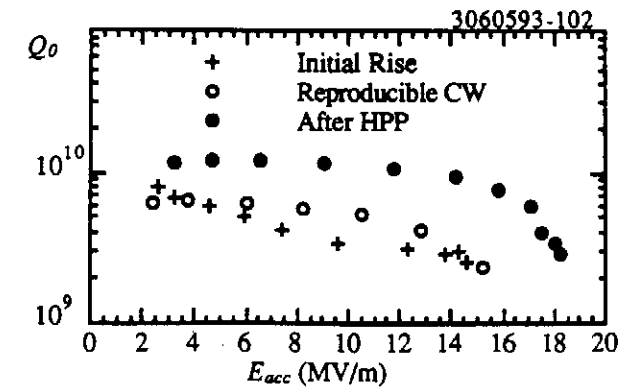

Figure 7. Q_0 vs. E_{acc} plots showing nine-cell cavity behavior before from the first vacuum accident.

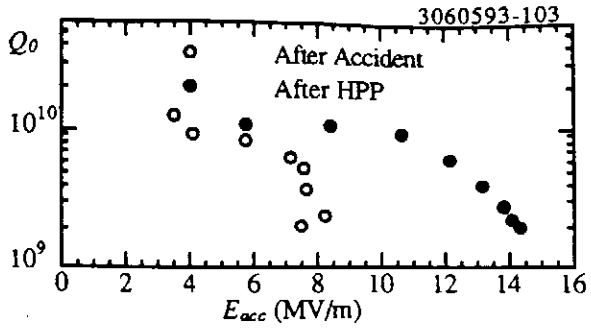

Figure 8. Q_0 vs. E_{acc} plots showing nine-cell cavity behavior before from the first vacuum accident.

The second event to be reported was an intentional test of a vacuum accident. Following the above described test, the cavity was cycled to room temperature, re-cooled, and re-tested. Then, while the cavity was at liquid helium temperature, the cavity interior was exposed to unfiltered atmosphere. The cavity was then remeasured, showing heavy field emission, as well as a low field Q_0 degradation. Following a room temperature cycle, the cavity was HPP processed, with peak power up to 105 kW, and fields up to E_{peak} = 42 MV/m. Again, partial recovery was made via HPP processing. All Q_0 vs. E_{acc} curves for this experiment are shown in Figure 8.

Based on these results, we conclude that if cavities are damaged by vacuum accidents, the performance may be regained through HPP RF processing, and sometimes with low power.

V. REFERENCES

1 *Proc. of the 1st TESLA Workshop*, Cornell University, Ithaca, NY, CLNS **90-1029** (1990).

2 J. Graber, et al., *Proc. of the 5th Workshop on RF Superconductivity*, D.Proch ed., DESY, Hamburg, Germany, **DESY M-92-01**, 576 (1992).

3 J. Graber, et al., *Proc. of the 1991 Particle Accelerator Conference*, IEEE Cat. No. **91CH3038-7**, 2411 (1991).

4 J. Graber, Ph.D. Dissertation, Cornell University (1993).

5 J. Graber, et al., this conference, poster Sa43.

6 J. Graber, et al., this conference, poster Sa44.

7 K. Shepard, Argonne Nat. Lab., priv. comm.

8 Q. S. Shu, et al., *IEEE Trans. Mag.*, **MAG-25**, 1868 (1985).

9 P. Schmueser, et al., **SRF 921117-10** (1992).

10 Ph. Niedermann, Ph.D. Thesis No. 2197, U. of Geneva (1986).

CLNS 93/1209
Presented at the 1993 Particle Accelerator Conference, May 17-20, 1993, Washington, D.C.

Status and Outlook for High Power Processing of 1.3 GHz TESLA Multicell Cavities,*

J. KIRCHGESSNER, P. BARNES, L. BARTELSON†, M. CHAMPION†, C. CRAWFORD†, H. EDWARDS†, J. GRABER, K. KOEPKE†, M. KUCHNIR†, A. MATHEISEN††, D. METZGER, D. MOFFAT, H. MULLER, H. PADAMSEE, M. PEKELER††, H. PFEFFER†, P. SCHMÜSER††, J. SEARS , and M. TIGNER
Laboratory of Nuclear Studies, Cornell University, Ithaca, NY 14853 USA

SUMMARY

In order to increase the usable accelerating gradient in Superconducting TESLA cavities, the field emission threshold barrier must be raised. As has been previously demonstrated on S-Band cavities, a way to accomplish this is with the use of high peak power RF processing. A transmitter with a peak power of 2 Mwatt and 300 μsec pulse length has been assembled and has been used to process TESLA cavities. Several five cell TESLA cavities at 1.3 GHz have been manufactured for this purpose. This transmitter and the cavities will be described and the results of the tests will be presented.

INTRODUCTION

High pulsed power processing (HPP) has been proved to be an effective method to overcome field emission in SC cavities. Many experiments done with 1-cell, 2-cell and 9-cell cavities at 3 GHz are discussed in other papers at this conference. The salient results of these experiments are:

1) Accelerating fields between 15-20 MV/m were reached with two 9-cell cavities (3 GHz) in 7 consecutive tests. For each test the surface of the cavity was prepared anew. In each case, heavy field emission was successfully processed with HPP to reach the final field levels. The low power Q was undamaged from HPP, so damage is not a concern.

2) The effectiveness of the processing depends clearly on the highest surface electric field reached during the pulsed processing stage. The highest pulsed surface field reached was 72 MV/m for a 1-cell, and 60 MV/m for a 9-cell. Power levels up to 50 kwatts were used for 1-cells and up to 200 kwatts for 9-cells.

3) In 9-cell cavities, field emission was completely eliminated for field levels up to $E_{cw} = 0.5\ E_{pulsed}$. If field emission is tolerated till the Q falls to about $5x10^9$, then higher fields can be reached, typically : $E_{cw} = 0.60\ E_{pulsed}$.

4) Processing takes place by an explosive mechanism. Dissection of processed cavities shows 1 - 10 μm size molten craters with traces of the original contaminants responsible for the field emission.

5) The processing is effective against new field emission when additional contaminants are introduced, such as by vacuum accidents.

6) During processing the Q falls to between 10^7 and 10^6.

7) It is possible, during pulsed operation, to exceed the field at which cw thermal breakdown is encountered; but then there is a strong competetion for the applied high power between field emission losses for processing and the growth of the normal conducting region(s). The method is, therefore, ultimately limited by breakdown, initiated by the maximum surface magnetic field. A low H_{pk}/E_{acc} ratio and a high RRR are, therefore, advised.

8) In a special 2-cell cavity with reduced magnetic surface field, it was possible to reach a surface electric field of 113 MV/m pulsed, and 100 MV/m cw, corresponding to a world record accelerating field of 34.6 MV/m.

EQUIPMENT FOR HPP AT 1.3 GHZ TESLA CAVITIES

Needed Power

For TESLA, the RF frequency chosen is 1.3 GHz, and the structure is a 9-cell with length 1.038 meters and $E_{pk}/E_{acc} = 2.1$. It is desired to eventually reach 25 MV/m accelerating, or $E_{pk} = 53$ MV/m at a Q of $5x10^9$. To determine the peak power we need to apply, we are guided by the results from our 3 GHz HPP experiments. If we can expect, $E_{cw} = 0.6\ E_{pulsed}$ after HPP, with some field emision still present, we need to be prepared to reach more than 90 MV/m surface field pulsed. We must also be prepared for the Q_0 to fall to $2x10^6$ during HPP. The pulse length over which the field can be built up during the pulse is a very important parameter in assessing the power. Fig. 1 shows that the needed peak surface field can be reached with 1 Mwatt of power and pulse length of 1 msec.

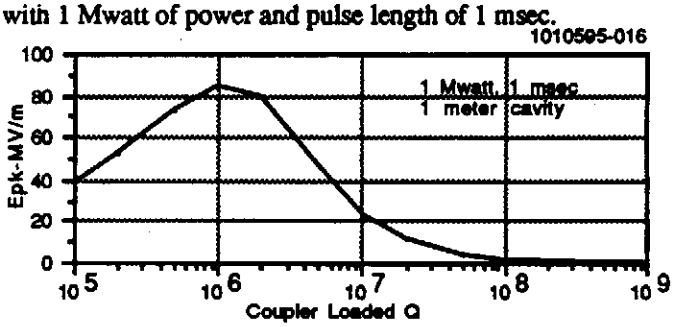

Fig. 1.

Klystron and Modulator

While preparations are proceeding for installation of SRF infrastructure and a TESLA TEST FACILITY at DESY, a

*Supported by the National Science Foundation, with supplementary support under the U. S. -Japan Agreement.
†FNAL
†† DESY, Hamburg, Germany

program has been launched at Cornell to test HPP at 1.3 GHz as soon as possible. The Boeing Defense and Space Group kindly agreed to lend us a klystron (Thompson TH2104) and PFN modulator. The system is intrinsically capable of 10 MWatts peak at 200 μsec with 185 Kvolts, or 5 Mwatts at 300 μsec. With commercial constant charge, constant current regulated pulsed capacitor charging supplies, we were successful in providing 110 KV to the klystron to obtain uniform 200 μsec long pulses of 2 MWatt peak power. The klystron and modulator system as installed at Cornell are shown in Fig. 2.

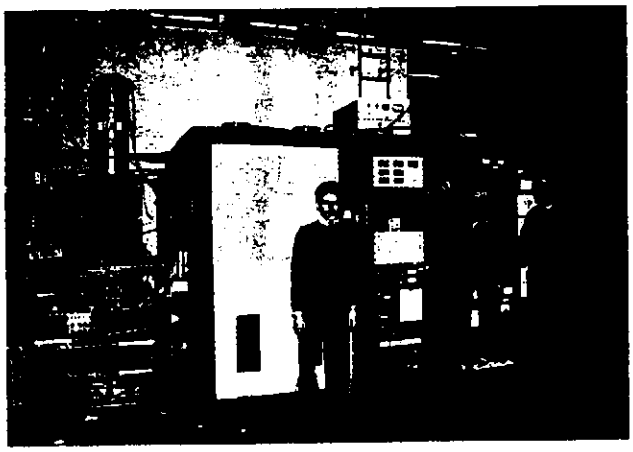

Fig. 2.

Niobium cavities

We decided to fabricate and test 5-cell structures instead of the final 9-cell structures for two important reasons: a) The available klystron/modulator operates at a maximum pulse length of 300 μsecs, b) The existing SRF facilities at Cornell (chemical treatment, shielded cold test area, furnace, clean rooms, etc.) are not of the appropriate size to handle a 1 meter long cavity. Fig. 3 shows the expected peak field that can be reached with 1 Mwatt of power and a 5-cell cavity at the available pulse length.

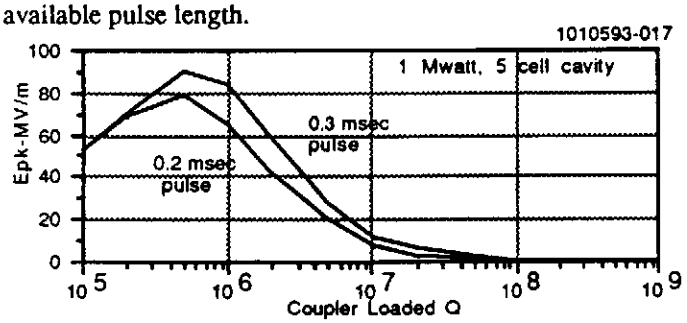

Fig. 3

Two 5-cell Nb cavities of the TESLA shape were built at Cornell. The accelerating mode properties of the cavity are listed in Table 1

Frequency	1308 MHz
R/Q	1088 Ω/m
E_p/E_{acc}	2.1
H_p/E_{acc}	42 Oe/MV/m

Table 1.

The cells are polarized as shown in Fig. 4 so that eventually a single HOM coupler can damp both polarizations of dipole higher order modes. The measured splitting for the dominant dipole modes was 13 MHz (TE_{111}) and 50 MHz (TM_{110}) modes. Fig. 5 shows a complete structure installed in the chemical treatment facility. One 2-cell and two 1-cell Nb cavities were also built. The RRR of the Nb used to fabricate these cavities was between 250 and 300. Copper cavites were also built to test the dies and fixtures.

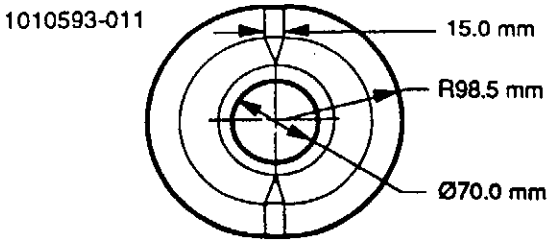

Fig. 4

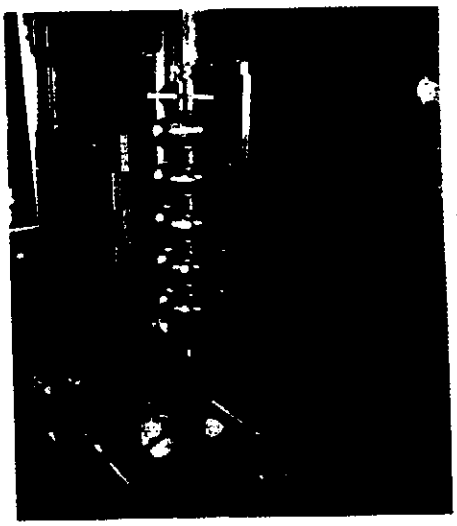

Fig. 5

1.3 GHz HPP Test Set Up

A high power cold test set up shown in Fig. 6 was built. The high power enters the cryostat top plate (not shown) through a WR650 reduced height waveguide. A room temperature teflon window above the top plate allows a vacuum in the waveguide. Near the bottom of the cryostat is a waveguide to coax doorknob transition, with an integrated cylindrical ceramic window to isolate the high vacuum, cavity region. The window was coated with TiN to reduce the secondary emisison coefficient. After fabrication, the VSWR of the input coupler was less than 1.6 between 1280 and 1320 MHz. The penetration of the antenna into the cavity is adjustable by a copper plated hydroformed bellow in the outer conductor. Q_{ext} can be changed from 10^5 to 10^{10} with 4" of travel. The slotted region of the outer conductor just above the doorknob is connected to the cavity vacuum pumping line. To check the microwave performance of the coupler, the BCS Q at 4.2 K of a 1.3 GHz Nb cavity was measured and verified for different positions of the antenna.

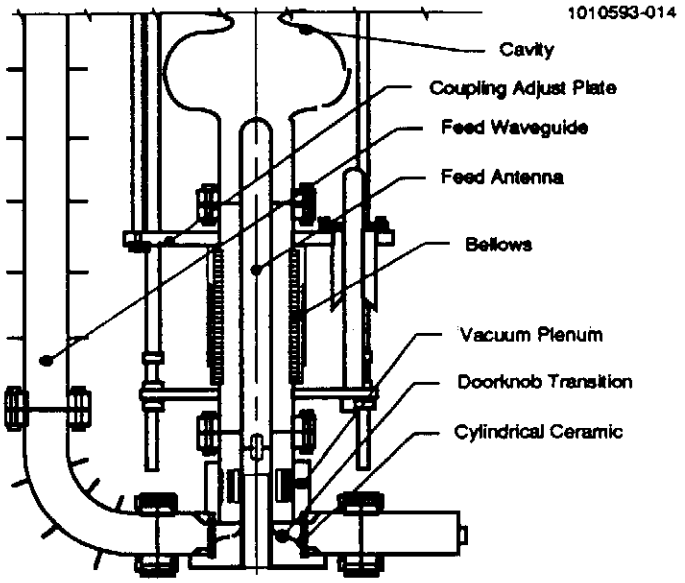

Fig.6

COLD TEST RESULTS

One problem is that the top of a 5-cell cavity stands at about 70% of the useable liquid helium reservoir height. Even with several batch fill and pump down iterations, it was difficult to keep the cavity completely under liquid at 2 K. A good solution to this problem was to pump down a 500 litre storage dewar to 2.2 K and then transfer 2.2 K liquid across into the test cryostat. By this method the running time at 2 K could be extended by many hours. While this solution was still being developed, it was decided to test the HPP method with the 2-cell cavity.

Fig. 7 shows three Q vs E curves for the test of the 2-cell cavity

a) The initial cw test with low power

b) after conditioning with cw low power only

c) after HPP up to 320 kwatts, 200 msec, maximum field 67 MV/m.

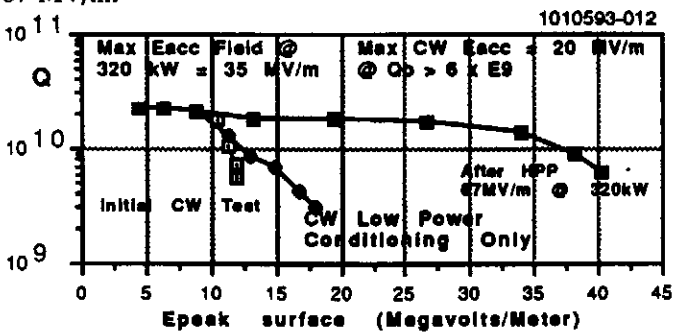

Fig.7

During pulsed power application, the maximum peak surface electric field reached was 67 MV/m.

The 2-cell result confirms many of the aspects of HPP that were proved in the 3 GHz program. Field emission was successfully processed away without damaging the low power Q. The maximum field reached during the pulsed stage shows, as expected, that the Q fell to about 2×10^6. The predicted E_{pk} was 70 MV/m for a 2-cell cavity, on applying 320 kwatts (200 μsec) and assuming that the Q_0 during processing fell to 2×10^6. The maximum predicted field is very close to the experimental result (67 MV/m). The field level E_{cw} at which the Q from field emission drops to 6×10^9 is 0.6 E_{pulsed}.

After the helium level problem was brought under control, a 5-cell cavity was tested. Unfortunately, due to reasons not yet understood, the preparation was not as clean as we desired. Both the low power Q and the field emission threshold were significantly lower than our usual results. Fig. 8 shows three Q vs. E curves. Although the initial field emission was heavy at 4 MV/m accelerating, with HPP we were still able to process and reach about 10 MV/m accelerating. The maximum power applied was 300 kwatts, at which power the E_{pk} reached during the pulsed stage was 40 MV/m. Again this implies that the Q fell to about 2×10^6 during HPP. We were not able to couple more than 300 kwatts because we encountered severe breakdown in the coupler.

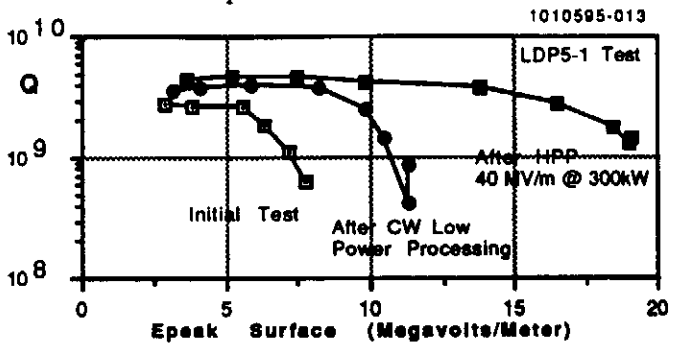

Fig.8

Two types of coupler conditioning events were seen in the 1.3 GHz HPP coupler. Between 10 and 300 kwatts the first type, called the staircase, was usually accompanied by severe vacuum degradation in the waveguide region. After some conditioning, it was possible to process this type of event, with improvement in vacuum and the return of the transmitted rf power signal to the expected exponential decay. The staircase event would restart on raising the power. Above 300 kwatt, a second type of coupler event was encountered. Nearly all the power was absorbed or reflected, so that very little power could be coupled to the cavity. Studies are in progress to determine the location of the coupler troubles. So far, the teflon window is exonerated, so the problem is originating from the cold end, i.e. the window/doorknob/coax/bellows area.

CONCLUSIONS

All the equipment necessary to test HPP at 1.3 GHz has been completed, installed and tested: 2 Mwatt klystron, 200 μsec pulse length modulator, high power test stand, and several multi-cell niobium cavities. The first test of HPP at 1.3 GHz shows that the technique works against field emission as expected, E_{acc} = 20 MV/m was reached. The processing power levels needed are as predicted from 3 GHz experiments. Understanding the limitations of the coupler is the next step to overcome the present 300 kwatt limit.

Presented at the 1993 Particle Accelerator Conference, May 17-20, 1993, Washington, D.C.

A Statistical Model for Field Emission in Superconducting Cavities*

H. PADAMSEE, K. GREEN, W. JOST, B. WRIGHT
Laboratory of Nuclear Studies, Cornell University, Ithaca, NY 14853 USA

SUMMARY

A statistical model is used to account for several features of performance of an ensemble of superconducting cavities. The input parameters are: the number of emitters/area, a distribution function for emitter β values, a distribution function for emissive areas, and a processing threshold. The power deposited by emitters is calculated from the field emission current and electron impact energy. The model can successfully account for the fraction of tests that reach the maximum field Epk in an ensemble of cavities, for eg, 1-cells @ 3 GHz or 5-cells @ 1.5 GHz. The model is used to predict the level of power needed to successfully process cavities of various surface areas with high pulsed power processing (HPP).

INTRODUCTION

Field emission is the most important gradient limiting mechanism operative in SRF cavities. Over the last 5 years, a large amount of data has accumulated on the performance of cavities limited by field emission. At the same time, there have been significant advances in understanding of the nature of field emission, the Fowler Nordheim (FN) properties of field emitters, their density of occurrence and their microscopic nature. Significant advances have also been forthcoming in understanding the nature of processing. Field emission currents increase with increasing field to initiate a microdischarge. This is an explosive event that leaves behind molten craters, surrounded by starburst shape patterns[1]. We present here a statistical model that encompasses a large body of known data on emitter properties to simulate a variety of features about the known behavior of SRF cavities limited by field emission.

*Supported by the National Science Foundation, with supplementary support under the U. S. -Japan Agreement.

THE MODEL

The surface of a SC cavity is divided up into a large number of segments (typically 20 per cell). Each segment i is sprinkled with a random number of emitters n_i, proportional to the surface area of the segment. The maximum emitter density, $n_i/area_i$ is the one free parameter of the model. As is well known from DC and RF studies of field emisison, the FN properties (β and emissive area S) can fall within a range of values; typically β is between 40 - 600, and log S (m^2) is between -8 and -16. We also chose β and S randomly, but the distributions for β and S values were chosen to mimic observed distributions from DC field emission studies[2]. Accordingly, (see Fig.1)

$N(b) \sim \exp(-.01*\beta)$
N(Log S) is a gaussian with half width of 2

After chosing an emitter set, we calculated at a given operating field, the trajectories of the emanating electrons and determined the power deposited on the wall of the cavity by the impacting electrons according to established techniques[3]. We then compare the total power for all emitters to the available CW rf power. For example, 10 watts for a 1-cell 3 GHz cavity, or 100 watts for a 5-cell 1.5 GHz cavity. If the simulated total power is less than the available rf power, the test is declared a "success". As a final feature, if the power deposited by a single emitter exceeds 100 watts, that emitter is declared to be processed and extinguished. The cut-off value corresponds reasonably with the recent discovery that when the total field emission current drawn from an emitter exceeds 10 mA, there is a significant processing factor[4].

RESULTS

By choosing 0.3 emitters/cm^2 for the single free parameter, we show in Fig. 1 the simulated performance for several sets of cavities: 1-cell @ 3 GHz, 1-cell @ 1.5 GHz and 5-cell @ 1.5 GHz. We calculate the fraction of cavities that "successfully" reach a field value, given by Epk. The simulated resluts are compared to the data from 100 tests at Los Alamos on 1-cells @ 3 GHz[5], 25 tests at Cornell on 1-cells at 1.5 GHz[6], and 100 tests at CEBAF on 5-cells at 1.5 GHz[7]. All data used are from cavities prepared by nominally the same standard chemical treatment. No advanced treatment data are used (eg. heat treatment or high pressure rinsing or high pulsed rf power processing).

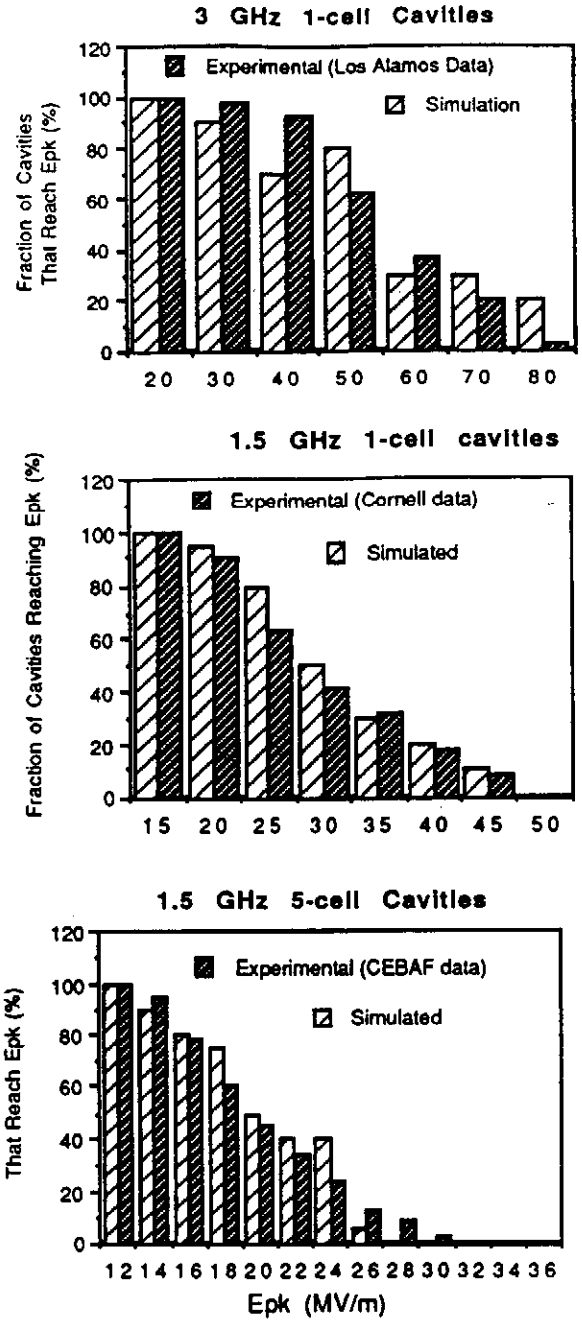

Fig. 1: Comparison between model and experiments

We see remarkable agreement betweeen simulations and data over the 3 sets of data. The most important feature is that, as the area of cavities increases, the successful fraction of cavities at a desired field level decreases. Note that the 5-cell 1.5 GHz cavites have 20 times the surface area of the 1-cell 3Ghz cavities.

Fig. 2 compares the measured and simulated β distributions from 1-cell, 1.5 GHz Cornell cavity data. Measured β values were obtained from thermometry data[6].

Fig. 3 shows the location of processed emitter sites for a 1-cell 3 GHz cavity operated at 80 MV/m surface field.

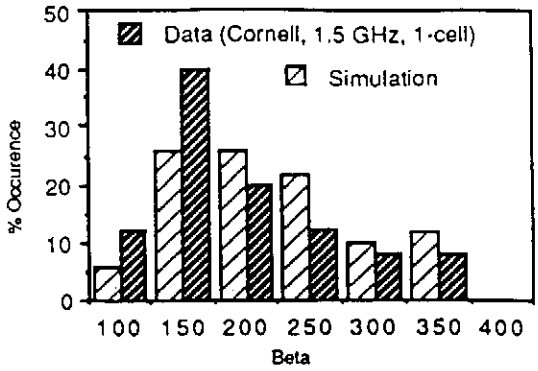

Fig. 2: Comparison between model and experiment

The distribution of processed emitter location corresponds well to the surface electric field, and compares favorably with the observed distribution of processed emitter sites (starbursts/molten craters) reported in [8].

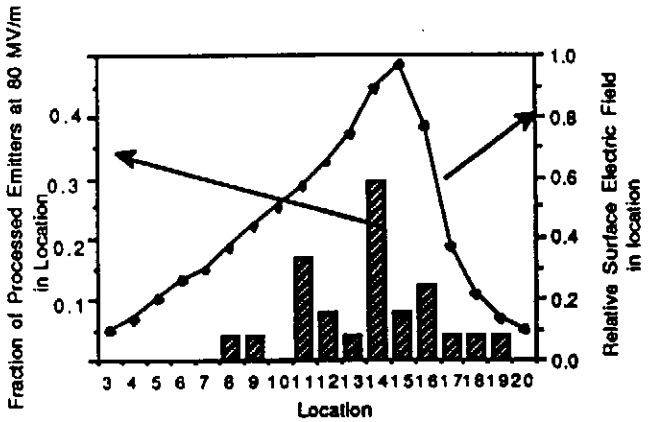

Fig. 3: Model predictions for location of processed emitters

The agreements obtained so far encourage us to examine the predictions of the statistical model for effectivenes of HPP (high pulsed rf power processing). We determine the behavior of a cavity at Epk = 40 MV/m, after it is processed at fields of 50, 60, 70 and 80 MV/m each. Table shows a list of emitters encountered in a 1-cell 3 GHz cavity at Epk = 40 MV/m. Because of the power into field emission the Q would drop to $5x10^8$. After processing at 50 MV/m and returning to 40 MV/m, some of the emitters are predicted to process. The remaining emitters and their deposited power are listed under the column headed 50 MV/m. The Q would rise to $3x10^9$. Note that the power and Q are re-calculated at the operating field of 40 MV/m. Similarly the result of processing at 60, 70 and 80 MV/m are listed under the appropriate columns. Again the predicted deposited power and Q are re-calculated at 40 MV/m.

The statistical model confirms that, for CW operation at Epk = 40 MV/m and with no field emission, it is necessary to carry out HPP at 80 MV/m. i.e [8]

Ecw = 0.5 Epulsed

Table 1: Single Cell 3GHz Monte Carlo HPP

Process at E (MV/m)	40		50		60	70	80
Watts at 40 MV/m for Run No. 1	5.8	25.9	5.8	0	5.8	5.8	0
2	8.5	0.6	0	8.5	0.6	0	0
3	23.3	1.6	0	1.6	1.6	0	0
4	0		0	0	0	0	0
5	78		0	0	0	0	0
6	1.7	3.6	5.3	1.7	0	0	0
7	3.9	0.3	0	1.3	0	0	0
8	1.5		1.5		1.5	0	0
9	18		0		0	0	0
10	7.5	0.6	0.6	0.6	0.6	0.6	0
Average power for one run (watt)	18.1		2.7		1.01	0.64	0
Q_0 at 40 MV/m	5.5×10^8		3.1×10^9		10^{10}	2×10^{10}	$> 10^{11}$

We carried out a similar evaluation for HPP on 1.5 GHz, 10-cell cavities, close to TESLA type cavities. We found that the relationship between Ecw and Epulsed is preserved. At Eacc = 12 MV/m, we first found that the Q would be lowered to 8×10^8 because of field emission. Only 5 emitters/cavity would be successfully processed. If HPP were carried out to establish a surface Eacc = 40 MV/m, then 110 emitters would be processed, and there would be no remaining field emission visible at Eacc = 20 MV/m. At Eacc = 25 MV/m, the Q would be lowered to 5×10^{10}. Hence the statistical model predicts that if TESLA cavities could be prepared with standard chemistry as the cavities today, it will be possible to reach the TESLA goal, provided HPP conditions could establish Eacc = 40 MV/m or Epk = 80 MV/m, if only for a short period, even μsecs[1]. Another work has shown[9] that a klystron and coupler that could provide pulsed power of 1 Mwatt for a pulse length of 1 msec would be sufficient to establish the desired field, even if the Q would fall to 2×10^6 during HPP.

CONCLUSIONS

A simple statistical model using known data about emitters can explain the behavior of SRF cavities when they are limited by field emisison. The model can be used to predict the requirements for HPP.

REFERENCES

[1] D. Moffat, et al. Part. Accel. 40:85 (1992)
[2] Ph. Niedermann, PhD thesis. Univ. of Geneva. 2197 (1986)
[3] H. Piel, Proc. of the 1st Workshop on RF Superconductivity, ed. M Kuntze. Karlsruhe: KFK. KFK-3019:145 (1980), p. 85
[4] J. Graber, PhD Thesis, Cornell University (1993).
[5] B. Rusnak et al, 1992 Linear Accel. Conf. Proc., p.728 (1992)
[6] H. Padamsee, et al. Proc. of the 4th Workshop on RF Superconductivity, KEK Rep. 89-21:445 (1990), p. 207.
[7] W. Schneider, CEBAF, private communication.
[8] J. Graber et al, this conference.
[9] J. Kirchgessner et al, this conference.

Presented as Poster Sa43 at the 1993 Particle Accelerator Conference, Washington DC, May 1993. CLNS 93/1216

Microscopic Investigation of RF Surfaces of 3 GHz Niobium Accelerator Cavities Following RF Processing*

J. Graber‡, P. Barnes, T. Flynn, J. Kirchgessner, J. Knobloch, D. Moffat, H. Muller, H. Padamsee, and J. Sears
F.R. Newman Laboratory of Nuclear Studies
Cornell University
Ithaca, NY 14853 USA

Abstract

RF processing of Superconducting accelerating cavities is achieved through a change in the electron field emission (FE) characteristics of the RF surface. We have examined the RF surfaces of several single-cell 3 GHz cavities, following RF processing, in a Scanning Electron Microscope (SEM). The RF processing sessions included both High Peak Power ($P \leq$ 50 kW) pulsed processing, and low power ($\leq$ 20 W) continuous wave processing. The experimental apparatus also included a thermometer array on the cavity outer wall, allowing temperature maps to characterize the emission before and after RF processing gains. Multiple sites have been located in cavities which showed improvements in cavity behavior due to RF processing. Several SEM-located sites can be correlated with changes in thermometer signals, indicating a direct relationship between the surface site and emission reduction due to RF processing. Information gained from the SEM investigations and thermometry are used to enhance the theoretical model of RF processing.

I. INTRODUCTION

The HPP experimental program was initiated in order to investigate high power RF processing as a method of reducing and understanding field emission in superconducting accelerator cavities. Results of this program have been presented at previous and present Particle Accelerator Conferences.[1],[2] An extensive description of the entire HPP program can be found in the recently completed Ph.D. dissertation associated with this work.[3]

We report here on the effort to characterize the microscopic effects of RF processing. Surface investigation studies of the cavities in the HPP program was initiated with the goal of finding physical evidence of processing on the RF surface. We were encouraged by the findings of the Mushroom cavity project[4] at Cornell, in which a specially designed, nonaccelerating cavity was examined in a Scanning Electron Microscope (SEM) following RF cold tests. Multiple phenomena were encountered in the high electric field regions of the cavity, indicating a strong link to field emission activity.

In order to better establish the link between surface features and RF processing, the experimental apparatus included an array of 100 thermometers placed in ten boards of ten resistors, spaced at 36 degree intervals around the azimuth of the cavity. Thermometers such as these have been a common diagnostic tool in SRF work for the last ten years.

SEM investigation of the cavities involves dissection of the single cell cavities in order to facilitate investigation of the RF surface, and is the final step performed on a test cavity.

II. PHYSICAL EVIDENCE OF RF PROCESSING

Ultimately it is desirable to gather microscopic information on field emission sites. DC field emission studies[5] have shown that these are micron or submicron features, for example, superficial particles. Even with guidance from thermometry, where the resolution is of the order of a few square millimeters, location of such minuscule features after dissection of a cavity presents a significant challenge. Fortunately, as this study shows, if the emission site processes, or undergoes significant change during cavity operation, then the additional features associated with the processing event make it substantially easier to locate the site.

Several sites were found which have both a significant thermometry signal, a change in signal after processing, and an associated surface feature. One example stands out above the rest, as the clearest processing event, therefore we will expand upon this site here. This site was found in a cavity (designated 1-5) which was RF tested specifically with the goal of limiting the run to one or two processing events. More examples of SEM located processing sites, as well as other phenomena can be found in references [3] and [6].

Figure 1 shows the Q_0 vs. E_{peak} plots from the three CW power rises of this experiment. The initial CW power rise was limited by heavy FE at E_{peak} = 32 MV/m. HPP processing was then performed with P_{RF} = 2 kW, t_{RF} = 630 μsec. Peak fields during processing reached 49 MV/m. The second CW measurement was limited at 34 MV/m, again by heavy FE. The second HPP session was performed with P_{RF} = 3.5 kW, t_{RF} = 630 μsec. Peak fields during processing reached 54 MV/m. In the final CW session, E_{peak} reached 36 MV/m, again limited by FE.

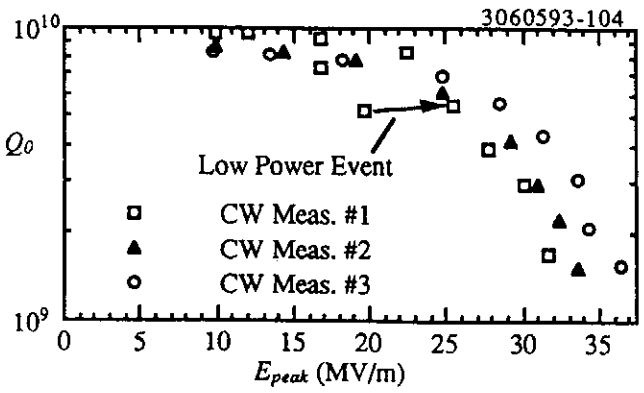

Figure 1. Q_0 vs. E_{peak} curves from low power measurements on single-cell cavity 1-5.

* Supported by the NSF with supplementary support from the U.S.-Japan Collaboration.

‡ Permanent Address: DESY, 85 Notkestrasse, 2000 Hamburg 52, Germany.

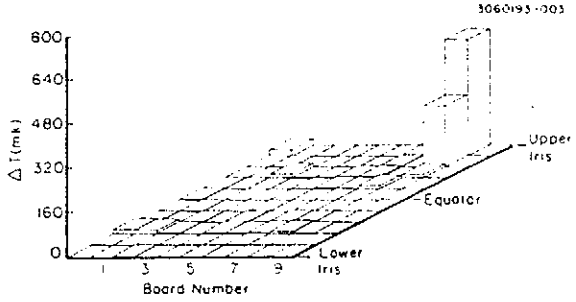

Figure 2. Temperature map measured at E_{peak} = 31 MV/m in the first CW power rise.

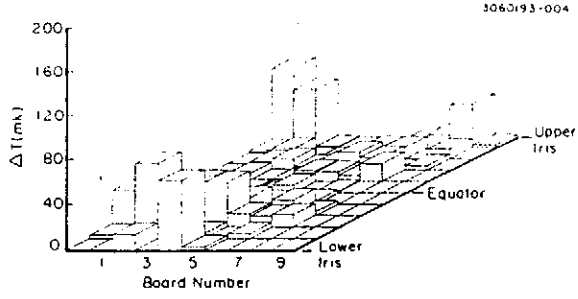

Figure 3. Temperature map measured at E_{peak} = 36 MV/m in the final CW power rise, following HPP processing.

Figure 2 is a temperature map of the cavity taken during the first CW measurements, at E_{peak} = 32 MV/m. The temperature map shows that the cavity was clearly dominated by a single emission site, located near the upper iris of the cavity board number 8. Figure 1 shows that, in addition to HPP processing, a processing event took place in the initial CW rise of the cavity, marked by the arrow. Inspection of the temperature maps reveal that this event was accompanied by a reduction in the heating at the dominant site shown in Figure 2.

Figure 3 is a temperature map taken during the final CW measurement, at E_{peak} = 36 MV/m. Note the reduced scale of the plot. While emission is still present, the site at the upper iris of board 8 is no longer dominating the cavity behavior. The change in heating is attributed to a change in FE characteristics through RF processing.

Given the measured change in heating, we then model the emission heating characteristics, before and after RF processing. In order to model the emission heating, we use a simulation[7] which assumes that the emission current is consistent with the enhanced Fowler-Nordheim (F-N) theory of emission:

$$I_{FN} = \frac{C A}{\phi} (\beta E)^2 \exp\left(-\frac{B \phi^{\frac{3}{2}}}{\beta E}\right) \qquad (1)$$

where I_{FN} is the FE current, E is the local surface electric field, ϕ is the work function of the metal, C and B are constants and β and A are the F-N field enhancement factor and emitter area, respectively. The present best model of the enhancement allows for both geometrical and material mechanisms of field enhancement. Furthermore, while no definite physical significance can be attributed to β or A, they are still useful quantities for characterizing the nature of emitters.

We therefore wish to extract values of β and A in order to better understand RF processing and its effect on emission

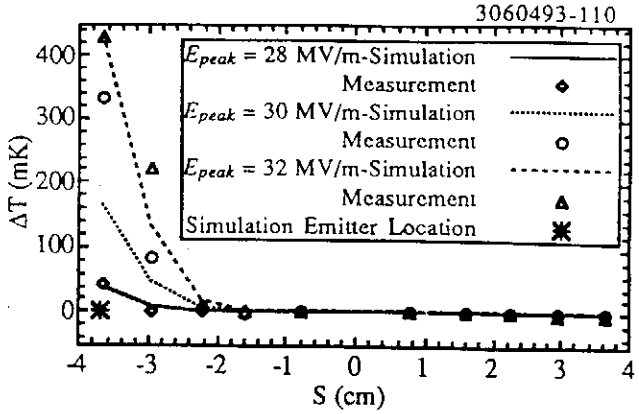

Figure 4. Comparison of measured and simulated temperature along board 8, in the first CW power rise.

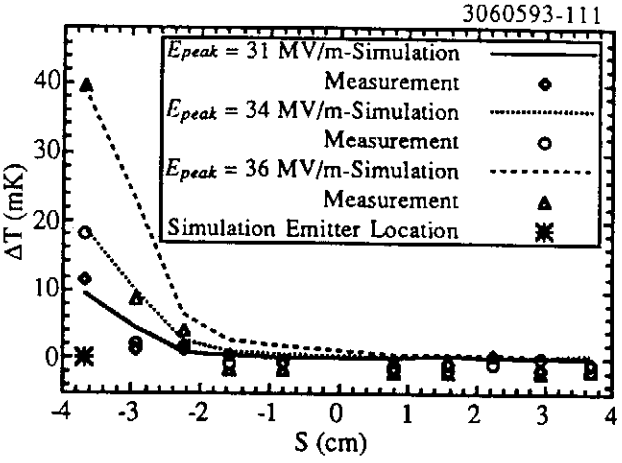

Figure 5. Comparison of measured and simulated temperature along board 8, in the final CW power rise.

sites. The method of extracting these values is to vary β and A in the simulation to best match the simulated with measured temperature signals on the cavity over several different electric field values. The field distribution of the fundamental mode of a cavity is such that emitted electrons follow trajectories with no azimuthal change, therefore all heating due to an emission site will be along a single board. S is the distance from the cavity equator along the cavity surface.

Figures 4 and 5 show the measured and simulated temperature signals along board 8 for the initial and final CW measurements on cavity 1-5, respectively. Simulation of the initial CW rise assumes the emission source at S = -3.7, β = 200, and $A = 3.2 \times 10^{-9}$ cm^2. The simulation of the final CW power rise assumes S = -3.7, β = 300, and $A = 1 \times 10^{-13}$ cm^2.

Given this agreement between measured and simulated thermometry, the cavity was dissected and put into the SEM, for examination in the region indicated as the processed emission site. The examination was successful, as one "starburst" feature was detected. Photographs of this starburst are shown in Figures 6 and 7. No other surface phenomena were detected in a position to eplain the change in emission characteristics.

As with most starbursts, the feature is dominated by a darkened (as viewed in the SEM) burst region, with diameter approxiamtely 200 microns. At the center of this starburst are

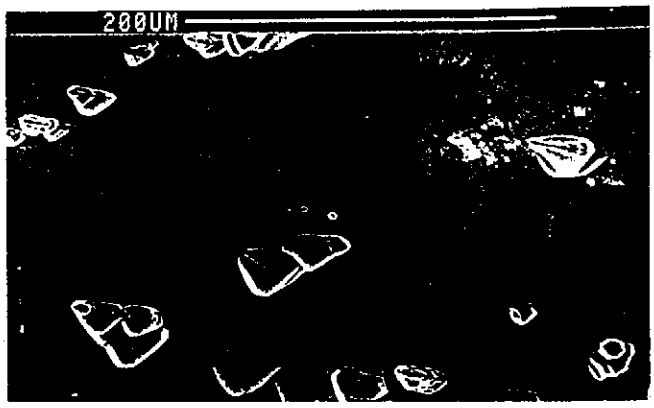

Figure 6. SEM photograph of the starburst region found in cavity S3C1-5. The starburst and craters are located in a position to explain the processing event.

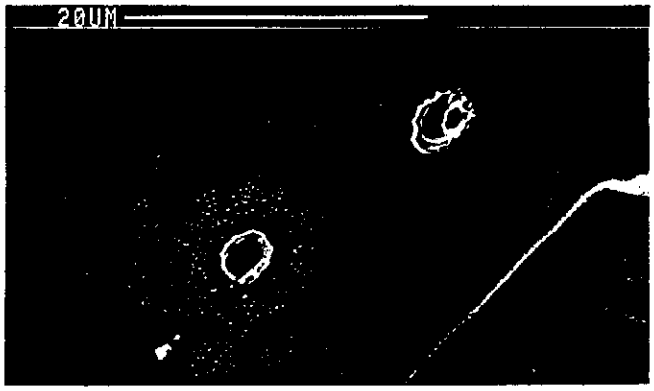

Figure 7. SEM photograph of the central region of Figure 6. Contaminant materials include Ca, Ti, C, and O.

several small (10 microns) crater regions, which appear to have become molten. The craters are shown in Figure 7.

The working model for RF processing, and the creation of a starburst is that as fields are increased, the emission current increases until the resistive losses become so high that the emitter melts/vaporizes. The event appears to be explosive in nature, as evidenced by the splash appearance of many crater regions. A more complete description of this model can be found in references [3] and [6].

Examination of X-ray information in the SEM indicate that contaminant materials at this site include Calcium, Carbon, Oxygen, and Titanium. The crystalline appearing features are called "etch pits," and are an pitting phenomena which occur frequently in cavities which are acid etched following high temperature baking. These pits appear throughout the cavity, and therefore are not thought to be significant to cavity behavior.

In all, we have examined 6 cavities following HPP processing. The general rule we have found is that the higher the fields that the cavity is exposed to, the more starbursts are found. This is consistent with the model presented above, as higher fields are capable of processing more sites.

This phenomena is demonstrated more conclusively, by examining the radial distribution of starbursts in the cavities. Figure 8 shows such a distribution, superimposed with the relative electric field as a function of radius and aligned with a

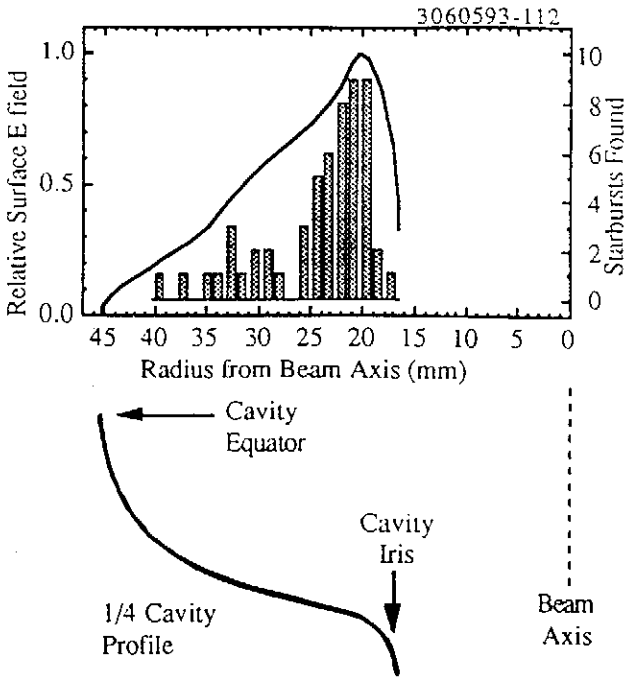

Figure 8. Radial distribution of "Starburst" phenomena found in all examined single-cell cavities, plotted along with relative surface electric field.

TABLE 1: CONTAMINANT ELEMENTS FOUND IN STARBURSTS IN HPP CAVITIES

Element	Starbursts	Element	Starbursts
Indium	19	Calcium	1
Iron	11	Silicon	1
Copper	4	Oxygen	1
Chromium	2	Carbon	1
Titanium	2		

quarter cavity profile. The starbursts are well concentrated in the high field region of the cavity, again supporting the model presented above.

Finally, in Table 1, we present a listing of the various contaminant materials detected in starburst in single-cell cavities.

III. ACKNOWLEDGMENTS

The authors thank Karen Sauer, Will Dickinson, and Adam Leibovich for their assistance on the thermometry portions of the HPP set-up.

IV. REFERENCES

1 J. Graber, et al., *Proc. of the 1991 Particle Accelerator Conference*, IEEE Cat. No. **91CH3038-7**, 2411 (1991).
2 J. Graber, et al., this conference, posters Sa42 and Sa44.
3 J. Graber, Ph.D. Dissertation, Cornell University (1993).
4 D. Moffat, Cornell Report **CLNS 90/991** (1990).
5 Ph. Niedermann, Ph.D. Thesis No. 2197, U. of Geneva (1986).
6 D. Moffat, et al., *Proc. of the 5th Workshop on RF Superconductivity*, D.Proch ed., DESY, Hamburg, Germany, **DESY M-92-01**, 245 (1992).
7 Cornell Report **CLNS/D 910121/24**, W. Hartung ed. (1989).

SRF Cavities for Future Applications

D. Proch
Deutsches Elektronen-Synchrotron DESY
Notkestraße 85, 2000 Hamburg 52, FRG

Abstract

Superconducting cavities are under operation or construction for acceleration of electrons and heavy ions at several laboratories. At present gradients around 5 MV/m, beam current up to 10 mA and operating experience exceeding 10,000 h are typical values. The advantage of superconducting RF is the high cw accelerating gradient, the low operating cost to establish RF voltage and the favourable cavity shape for a low loss factor. Ongoing progress in improving Niobium material, simplifying design and fabrication, understanding of performance limitations and investing cures against field emission promise to increase the operating gradient at reduced investment costs. High beam current applications are investigated to take advantage of the small higher order mode impedance. The most challenging development is the use of superconducting cavities for a TeV Linear Collider (TESLA).

I. INTRODUCTION

For more than ten years superconducting cavities are under use in accelerators. At several laboratories different types of low β cavities operate under routine conditions to boost the energy of heavy ions. They produce cw gradients above the capability of normalconducting resonators and work reliable and cost efficient. This paper deals with cavities designed for $\beta = 1$ applications. A recent review of low β superconducting cavities is given in [1].

Superconducting cavities are used to accelerate electrons in linacs (Darmstadt, Frascati, HEPL, JAERI, Saclay) and in storage rings (CERN, DESY, KEK). A recirculating linac with 160 m of superconducting cavities is under construction at CEBAF [2]. In total about 800 m of superconducting resonators are under operation or construction. Several 10^5 cavity-hours of operating experience demonstrate the mature character of this technology. Detailes of the experience gained at different laboratories can be found in [3]. Improvements are expected in raising the operating gradient, lowering fabrication costs and in reliability of auxiliary equipment (input- and HOM couplers, windows, etc).

In this paper recent developments and future projects are discussed.

II. RECENT PROGRESS IN CAVITY TECHNOLOGY

A. *Niobium material*

Superconducting cavities are produced from sheet material by electron beam welding. The mass production of Niobium has a high standard in respect to the purity of the bulk and the cleanliness of the surface. Considerable improvements have been gained in raising the thermal conductivity by further refinement during the melting processes. As measure of the (temperature dependent) thermal conductivity the value of RRR (Residual Resistance Ratio: $R_{300K}/R_{4.2K}$) is often quoted. Nb material with RRR = 300 is available in large quantities, an improvement by a factor of ten compared to that ten years ago. A high thermal conductivity stabilizes excessive heat flux, thus increasing the breakdown value of a quench.

A further increase of the thermal conductivity can be reached by Ti solid state gettering. The completed cavity is fired for several hours around 1400 ^0C together with some Ti material [4]. This purification process is especially valuable to heal mistakes during fabrication (e.g. bad vacuum in the e^-–welder). A maximum value of RRR 1000 at a cavity has been reported recently [5].

B. *Cleaning procedures*

Field emission is the main effect in limiting the accelerating gradient in superconducting cavities. The low AC-loss of a superconductor makes the cavity sensitive to any additional loss mechanism. Another consequence of field emission is the dark current in linacs. Dust particles (metallic or dielectric) on the surface are the most likely source of field emission although other "irregularities" or intrinsic surface properties cannot be completely excluded. Cleaning of the surface by chemistry (BCP: Buffered Chemical Polish) and thorough rinsing is essential to suppress field emission. An automized chemical cleaning facility has been

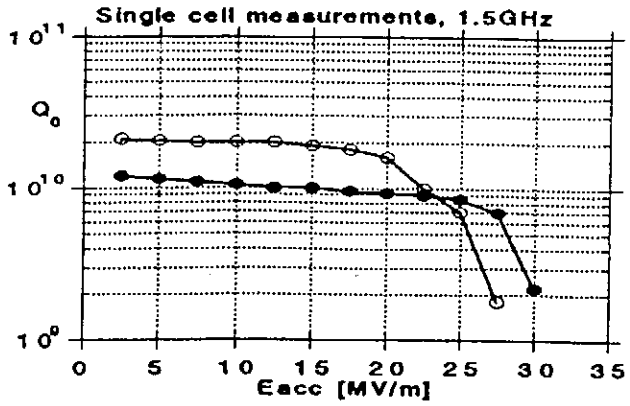

Figure 1: Measured results after application of thorough cleaning technique: (○) single cell (1.5 GHz) treated by automized chemistry [6], (●) single cell (1.5 GHz) treated by high pressure water rinsing [5]

established at Saclay [6]. The cavity undergoes a degreasing, BCP, rinsing and drying process under sealed off conditions. Several single cell cavities have been tested so far. Figure 1 shows a typical result: The cavity stays at a high Q value of 10^{10} and no field emission is seen until 20 MV/m. It has to be demonstrated that these exceptional properties can be gained at multicell cavities, too. A similar equipment is under construction at DESY to process 9 cell 1.3 GHz cavities [7].

Rinsing with high pressure water is another cleaning technique. First encouraging results on 350 MHz sputtered single cell cavities have been reported from CERN [8]. Recently single cell 1.5 GHz cavities have been treated several times at CEBAF [5]. Figure 1 shows a typical result: high gradients without field emission up to $E_{acc} = 25$ MV/m could be measured reproducibly.

C. *High power processing (HPP)*

In many experiments the onset of field emission is raised to some degree by operating the cavity at high field level (cw or pulsed). The time constant of a superconducting cavity and lack of RF power does not allow to reach higher fields under pulsed conditions in order to do more processing. At Cornell cavities have been HPP treated [10], similar test stands are under construction for 1.3 GHz 5 and 9 cell cavities at Cornell, FNAL, DESY. RF pulsed power (300 kW to 1 MW, 100 μs to 1 ms) and adjustable input coupler allow to reach high fields before thermal runaway occurs. Figure 2 shows the properties of 9 cell cavities before and after HPP. Further processing was limited by the available RF power. Thermometry and surface studies on these cavities and special demountable single cell resonators (mushroom cavity) [11] have been carried out in parallel. It is concluded that dust particles as possible field emitters are heated during the RF pulse to such an extent that they evaporate in a short time. One attractive feature of HPP is the possibility to apply in situ processing in the linac (to do processing after a dust accident, e.g.).

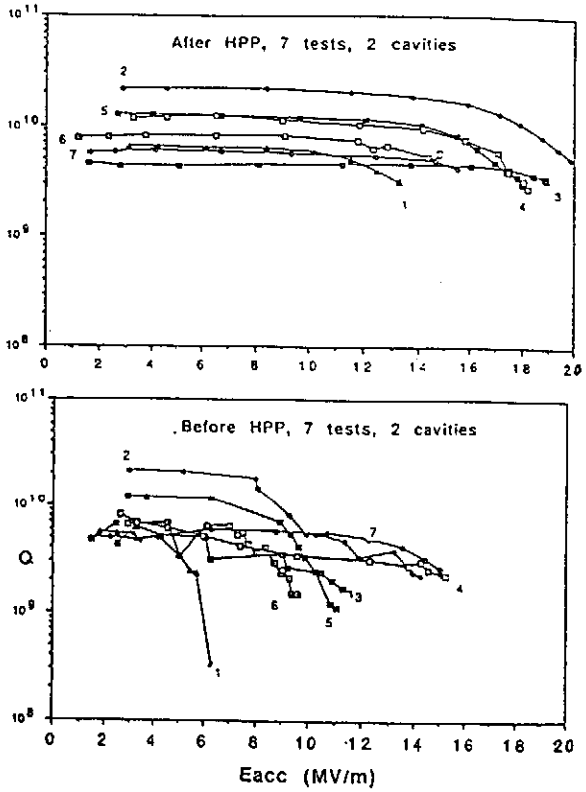

Figure 2: Measured results of 9 cell cavities (3 GHz) before and after HPP [10]

D. *Nb sputter technology*

At CERN the technology of Nb sputtering for cavities has been developed [12] and was transferred to industry. In total 150 4 cell cavities (350 MHz) are being produced at three companies [13]. The advantages of a sputtered cavity are

- cost saving of Nb material; this is especially true for large cavities at low frequencies,
- reduced surface resistance as compared to bulk Niobium and thus savings in operation costs,
- no need for a magnetic shielding against ambient field,
- stabilization of quench areas by the high thermal conductivity of Cu.

Figure 3 shows performance data of solid Nb and sputtered Nb cavities. It can be seen that sputtered cavities show enhanced Q values. The maximum fields E_{acc} reached are comparable.

E. *Field emission*

Ongoing experiments at Saclay [15] and Wuppertal [14] investigate the nature of field emission from Nb surfaces by scanning the surface with a needle under high DC voltage. At Saclay dust particles are produced on purpose and their field emission is characterized. An analysis of the large amount of data leads to the following conclusions [15]:

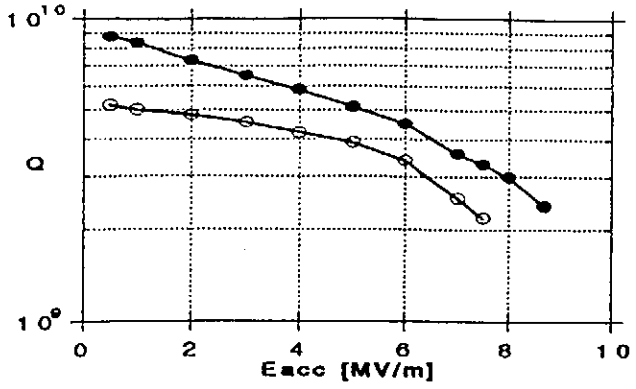

Figure 3: Measured result of 4 cell cavities (350 MHz) at acceptance test [13]: (o) average of 19 cavities made from solid Nb, (•) average of 14 cavities made by sputtered Nb on Cu

- field emitting sites could always be identified with dust particles,
- metallic dust particles emit at lower values of surface field than dielectric dust,
- there is no big influence of the underlying Nb_xO_y layer.

At Wuppertal clean Nb surfaces are investigated. Conclusions are [14]:

- most field emitting sites could not be identified with dust particles,
- very often the field emitting site is near to irregularities of the surface topology (etching pits?, etc.),
- after 1400^{0}C UHV bake out suface fields up to 100 MV/m could be achieved reproducibly without field emission,
- field emitters seem to reappear after heating at 600 – 800^0C.

It is not prooven, however, that field emission under DC voltage or RF fields is determined by the same processes. RF heating of a loose particle on the surface might initiate a thermal field emission. The benefit of HPP and the obvious evaporation of earlier field emitters indicate that for surface fields in the range of 20 to 50 MV/m dust particles might play a dominant role.

III. NEW DEVELOPMENTS

A. *RF power saving*

Saving of RF installation and operating cost by use of superconducting cavities is not a new argument. In the past this issue was often underestimated. Doubts about the reliability of superconducting RF accelerating systems prevailed. Operating experience at CERN, DESY and

	U(MV)	$P_{klys.}$ (MW)	P_{ac} (MW)
NC	81.3	3.4	5.66
SC	55.7	0.25	0.42
Cryogenic		(500 W at 4.2 K)	0.15
Tot.	**137.0**		6.23
NC	137.0	9.65	16.05
SC	-	-	-
Tot.	**137.0**	**9.65**	**16.05**
Energy			16.05
saving:			- 6.23
			9.82
saving: 4000 h × 9820 KW × 0.15 DM/KWh = 5.9 MDM			

Table 1: Operating conditions of the RF system in HERA e^- in 1992 (upper part). The part below shows the corresponding expenditures without superconducting RF and gives with the resulting energy savings (NC: Normalconducting, SC: Superconducting)

KEK demonstrates, however, that superconducting cavities work stable and reliable after overcoming difficulties with auxiliary equipment (HOM couplers, cables and connectors, proper synchrotron radiation shielding etc.) which, of course, need adequate attention. It is difficult to give a formula of investment and operating cost saving which covers any case of application. It also varies in case of new or supplementary installation. The operating conditions of the HERA normal– and superconducting RF system is given as example. The upper part of table 1 shows the operational data during the 1992 run. The lower part gives calculated data for the same circumferential voltage but without superconducting cavities.

B. *High current applications*

There is an increasing demand for superconducting cavities in future accelerators with high beam currents:

- reduced cavity-beam interaction by the intrinsic low value of the HOM loss factor of a typical superconducting cavity shape (no nose cones, large iris hole, low operating frequency),
- high gradient, thus reducing the number of cells needed (benefit for length and HOM impedance),
- saving of RF installation and operating costs.

One example of a high current design is the single cell cavity (500 MHz) developed at Cornell for use in a B–factory (CESR B) [16]. The principle layout is presented in Figure 4. The challenge of this design is the HOM damping scheme and the power rating of the input coupler. The higher order modes are damped by a lossy plating at the outer end of the beam pipe. This broad band damping

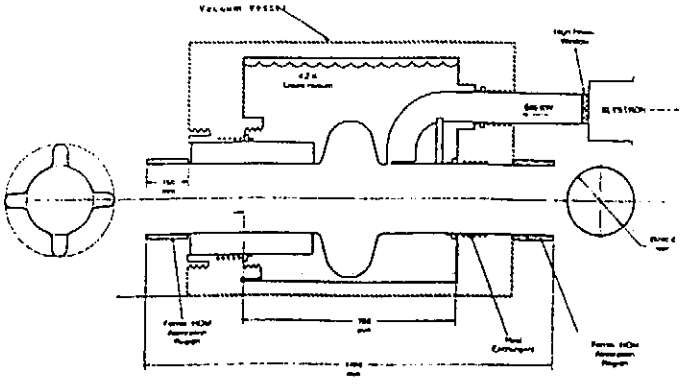

Figure 4: Principle layout of the single cell cavity (500 MHz) for use in a B-factory [17]

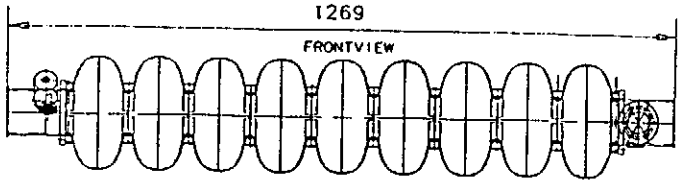

Figure 5: Cross section view of the TESLA 9 cell cavity (1.3 GHz) [7]

scheme is supplemented by a type of riged waveguide to transfer HOM energy below the cut off frequency of the beam pipe, too. High damping with equivalent Q values of around 100 could be measured with Cu models [17]. The input coupler consists of a rectangular waveguide with a coupling slot towards the cavity. First cold measurements demonstrated $E_{acc} = 10$ MV/m at Q value of 2×10^9 [18].

C. *High gradient applications*

Superconducting cavities have been proposed for linear colliders since some time [19]. An international collaboration has been formed to work on the design of TESLA [20] (TeV Superconducting Linear Accelerator) and to build a test facility [7]. Superconducting cavities allow storage of RF energy in a very efficient way. As consequence long RF pulses can be established at low frequencies (large cavities). The benefits for a linear collider are:

- low cavity loss factor, thus very relaxed alignment and vibration tolerances,
- long bunch to bunch distance,
- moderate RF peak power demand.

In order to reduce the total costs of TESLA substantial improvements are needed as compared to the state of the art of today:

- the investment costs of about 400 kDM/1 active m (HERA SRF), have to be reduced by a factor of about four,
- the operating gradient has to be raised above 20 MV/m.

In the following paragraphs ongoing and planned R & D effort is described.

1) *Cavity:* The shape of the cavity has to be optimized in respect to

- low value of E_{peak}/E_{acc} to suppress field emission,
- low loss factors $K_{\parallel}, K_{\perp}$ to reduce wake fields,
- high shunt impedance to reduce the refrigerator load,
- high cell to cell coupling to reduce tolerance sensitivity,
- low H_{peak}/E_{acc} values to suppress local heating,
- appropriate shaping to avoid trapped modes (with fields only in the middle cells thus having no damping by end cell couplers).

The elements of the cavity shape (iris ∅, curvature of equator and iris boundary) have different or even contradictory consequences to the above mentioned properties. There is no unique cavity design with the exception of a rounded (circular or elliptical) equator region to avoid multipacting. Figure 5 shows the shape of the TESLA cavity. A number of 9 cells per cavity has been choosen. More cells are desirable for economy reasons and might be possible. But sufficient HOM damping and avoiding trapped modes do not recommend an increase of this number without further detailed and time consuming studies. The low value of $E_{peak}/E_{acc} = 2$ is important to succeed in suppression of field emission.

The existence of trapped modes can be explained by a field flatness problem due to heavily detuned end cells (which are compensated for the fundamental mode). One way to overcome this problem is to detune the end cells even more but in an asymmetric way. Detuning one end cell sufficiently more than the other one results in a tilted field profile. As consequence one of the HOM couplers at each end of the cavity damps very effectively. Measurements on three 9 cell Cu cavities with these asymmetric end cells confirmed this idea [21]. It could be demonstrated, too, that the fundamental mode field pattern is undistorted by proper compensation.

At gradients of some 20 MV/m the cavity contour will be deformed and the resonant frequency is shifted by a noticeable value. This is due to the Lorentz force action of the electromagnetic fields to the surface currents. The iris region is bent inwards, the equator region is bent outwards, both result in a lower resonant frequency. Experimental values of 4 Hz per $(\mathrm{MV/m})^2$ have been reported [18].

FEM analysis of the 1.3 GHz TESLA cavity (wall thickness 2.8 mm) predicts about 1000 Hz shift at 25 MV/m [22]. This value has to be compared to the loaded bandwidth of 330 Hz. The proposed stiffening ring at the iris (see Figure 5) reduces the effect to 300 Hz, further reduction requires expensive stiffening schemes at the equator. Modulation of frequency and phase of the RF drive during filling the cavity has been proposed to reduce amplitude and phase variation during the beam pulse to an acceptable value [23].

A naive interpretation of the Brillouin diagram concludes that the slope and thus the group velocity of the π–mode is zero. It was investigated whether the energy withdrawn by one bunch can be restored within the 1 μs bunchdistance in the 9 cell standing wave cavity. The transient behaviour of a coupled resonator model was investigated by applying the Laplace transformation [21]. The result is that the field can be reestablished in each cell but that there are amplitude oscillations at the 10^{-3} level. This can be understood as beating patterns of the non-π mode excitations. The distortion of the energy resolution of the beam by this statistic effect needs more investigation.

2) *Cryostat:* Most savings in the linac costs can be gained by substantial improvements of the cryostat design. The present layout shows warm–cold transitions every few cavities, expensive distribution boxes and separate transfer lines. In the TESLA design a cavity string of 1700 m is cooled by one 10 kW, 1.8 K refrigerator. A 300 mm Ø suction line pumps the whole string to 1.8 K and is the mechanical support of the cavities at the same time. One integrated valve box every 144 m supplies LHe to the cavities. The smallest assembly unit is 12 m long, containing 8 cavities and one superconducting quadrupole. Figure 6 shows a cross section of the present layout. Each cavity is surrounded by its own He–tank; couplers and flanges are placed outside the LHe. Slow tuning is done by a motor and gear box at cold temperatures. A coaxial input coupler penetrates the vacuum vessel every 1.3 m. The power rating of the coupler is 200 kW beam power (1.5 ms) and up to 1 MW, 500 μs for in situ HPP.

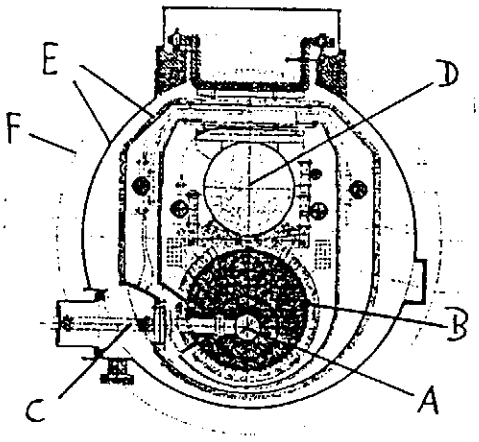

Figure 6: Cross section of the TESLA crystat: A: cavity, B:LHe vessel, C: input coupler, D: suction line, E:radiation shields, F: vacuum vessel.

ACKNOWLEDGEMENTS

The fruitful discussions and the fast exchange of experience with my colleagues from CEBAF, CERN, Cornell, DESY, Saclay and Wuppertal is gratefully acknowledged.

REFERENCES

[1] W. Weingarten, *Proc. XVth International Conference on High Energy Accelerators*, page 678

[2] A. Hutton, this conference

[3] F. Dylla, this conference

[4] P. Kneisel, *Journal of Less Common Metals*, page 139, 179 (1988)

[5] P. Kneisel, CEBAF *private communication*

[6] B. Bonin, *private communication*

[7] *TESLA-Report 93-01* (Available from DESY)

[8] Ph. Bernard et al., *Proc. of the 5th Workshop on RF Superconductivity*, Vol. 1, page 487 (1992)

[9] H. Padamsee et al., *Proc. of the 1991 PAC*, page 2420

[10] J.H. Graber, Cornell, *Dissertation*, May 1993

[11] Q.S. Shu et al., Cornell *CLNS-90/1005*

[12] C. Benvenuti, *ibid. ref. 8*, page 189

[13] G. Cavallari et al., this conference

[14] E. Mahner et al., *Applied Surface Science 67* pp. 23 - 28 (1993)

[15] M. Jimenez et al., *DAPNIA/SEA 02/93*, Saclay

[16] CESR-B, "Conceptual Design", *CLNS 91-1050*

[17] J. Kirchgessner et al., *Proc. of the 1992 Linac Conference*, Ottawa (1992)

[18] H. Padamsee, *private communication*

[19] M. Tigner, *Nuovo Cimento 37* (1965) page 1228

[20] H. Edwards, this conference

[21] J. Sekutowicz, DESY, *private communication*

[22] H. Kaiser, DESY, *private communication*

[23] H. Henke, B. Littmann *TESLA Report 93-12* (Available from DESY)

Progress Report on the TESLA TEST FACILITY

The TESLA Collaboration
reported by
H. T. Edwards
DESY/FNAL*

Abstract

An R&D RF cavity production and test program is underway to evaluate the practicality of superconducting RF cavity systems for future linear collider applications in the 500 Gev energy region. An international collaboration[1] organized by DESY is assembling a TESLA test facility to assess gradient, systems, and manufacturing cost issues of the superconducting RF collider option. Construction of a state of the art cavity processing facility is underway. It is proposed to build four 12 m long cryounits each with eight 9-cell superconducting cavities operating at 1.3 GHz. Two 4.5 Mwatt, 2 msec pulse length klystrons will distribute power to the total 32 cavities. An electron gun and injector section will be included in this test facility, and beam tests with energies of about 500 MeV will be carried out.

Introduction

There is wide spread consensus amoung the HEP community that an e^+e^- collider with a center-of-mass energy of 500 GeV and luminosity of a few time $10^{33} cm^{-2} sec^{-1}$ should be considered as the next accelerator after the SSC/LHC. Such a collider would provide for top analysis via $t - \bar{t}$ production and also have the potential for discovery such as Higgs with mass below ≈350 GeV.

Within the accelerator community a number of alternate linear collider design efforts are being pursued that meet the above stated energy and luminosity requirements. These designs have many features in common such as the overall linear collider/injector layout, but differ mainly in the choice of spot size, bunch charge and frequency. The differences mainly come down to a trade off between the amount of beam power that is accelerated vs the spot size which has to be provided at the interaction point. The greater beam intensity can be used to balance more relaxed beam emittance and final focusing requirements. Typically, bunch intensities vary by an order of magnitude and vertical spot sizes by more than that. Also the different designs span a variety of rf frequencies from 1.3 to 30 GHz.

The TESLA approach lies at the low frequency, high intensity end of the present parameter range.[2] The use of superconducting rf cavity structures aids in achieving the higher beam intensity design. The resulting beam power could as well be applied toward higher luminosity design values if more stringent emittance and focusing were employed. However the major appeal of the scrf approach is that it allows for the more relaxed tolarances and less ambitious extraploations from todays state of the art operation at SLC.

The technical advantages of the superconducting rf cavaties stem from their high Q values and low wall losses. This allows for the use of large aperture structures operating at relatively low frequency, with relatively long pulse lengths, and low peak rf power requirements. The large aperture of the cavities are perceived to be a major advantage as it results in substantially reduced wake effects for both longitudinal and transverse wake fields. (the longitudinal wake scales with the aperture (a) as $1/a^2$, and the transverse wake as $1/a^3$.) As the aperature of an L band sc cavity is ≈ 70mm diameter, or about ten times larger than in some of the higher frequency designs, relaxed linac alignment and vibration tolarances should result even with the large bunch charge contemplated. With the larger emittance, more dilution can be tolerated in the linac, in the optics after the linac and the final focus. In addition the focusing strength, optical quality and alignment needed is not so stringent because of the higher beam power and larger spot. The result for the detector is more longitudinal space after the last focusing element, a long beam pulse with considerable time between bunch interactions. Just how much easier the alignment/vibration and field quality tolarances will be and how favorable the result will be for the detectors, will require a serious design study employing all the knowledge that has been learned at SLC and with other collider design efforts.

Though the use of superconducting rf cavities appears to greatly reduce the overall technicial difficulty of a linear collider, the difficulty has been concentrated in the one area of the sc cavities themselves. Reliable accelerating gradients at the 20 - 30 MeV/m must be achieved in a cost effective cryogenic assembly. Conventional wisdom in the past has used 5MV/m for a reliable operating

*FNAL is operated by the Universities Research Association, Inc. for the U. S. Department of Energy

value of the gradient. Costs for production of a few cavities have been typically 200k$/m, or 40k$/MV. In order for the superconducting approach to become a viable alternative, this figure of merit must be reduced to the range of about 2k$/MV (or say 50k$ per meter with a gradient of 25MV/m). Though this would appear a somewhat daunting goal, it is to be noted that CEBAF is typically achieving averages of 12MV/m on their recent production. New cavity processing techniques such as heat treatment and high pulsed power rf processing show that gradients of 15 - 20 Mv/m can be reached in multi-cell structures. This work is reported in depth in other papers at this conference. Many tests on single cell cavities by the same techniques show accelerating gradients between 25 - 35 MV/m demonstrating that there are no fundamental limitations to the desired gradients for TESLA. Engineering design for economies of scale must be adressed as well, for whereas CEBAF for instance needs 360 cavities a linear collider would require typically 20,000. The goal of the TESLA R&D program is to build a test string of cavities of a modular design suitable for the linear collider application and to address the operating systems issues of the string as well as the all important gradient performance and cost effective design of the cavities and their cryostat. The goal is to have a 50m string of 32 cavities operational with beam in the 97 time scale and to be able to at that point make a rational judgement as to potential achieveable gradient and cost extrapolation to mass production scales.

The TESLA Test Facility (TTF)

The gradient goal of the R&D program is 15MV/m at Q's of 3×10^9. The long term collider design goal is 25MV/m at 5×10^9. Individual cavities are standing wave pi mode 9 cell structures; they are about one meter long and have individual coaxial input couplers and HOM couplers. Needed power for each cavity is 206kW at 25MV/m and 8ma of beam.

As cost savings is a major point of the R&D, it is important to come up with an efficient, simple, and reliable arrangement for the cavity cryostat. To this end, long cryomodules (12m) will be built which contain a linear array of 8 cavities with their associated input and HOM couplers. The end of each module near the interface will contain quad focusing, beam detectors, steering, and an annular space for high frequency HOM absorber cooled to 70K. The magnetic elements are superconducting and operate at 4K.

Each cavity has its own helium container, connected in series to the adjacent components. All vacuum flanges are arranged so there are no helium to vacuum flange interfaces but rather beam vacuum to cryostat vacuum, or cryostat vacuum to air. All helium to vacuum joints are welded. The input couplers are coaxial with two ceramic windows; one at 70K, the other at room temperature.These couplers have bellows which allow for an order of magnitude adjustment in the external Q, and for longitudinal thermal contraction of the cavity array over the length of the cryomodule.

The cavities are suspended and aligned off the large 300mm helium gas return pipe. The whole cryostat and shield arrangement is similar to the HERA or SSC magnet cryostats. Three support posts derived from the SSC posts provide the warm to cold support transition from the outside of the cryostat to the helium gas header[3].

The RF system will consist of two 4.5 MW modulators and Thomson Th2104 klystrons capable of 2ms RF pulse at 10 Hz. Each modulator is capable of providing 1.5 times the power needed for 16 cavities under full beam current and gradient (25MV/m).

One of these high power systems will also be used for RF processing at high peak power(HPP) of the individual cavities. It is expected that 1 MW RF levels will be required for HPP. An additional RF system will be used for the TTF injector.

A cryogenic system which supplies 200W at 1.8K and 200W at 5K is envisioned using an existing DESY refrigerator and an additional 1.8K cold box. The budgeted heat load at 1.8 and 4.5K respectively per meter is: static 0.4/1.25 W, total with rf power and beam 1.35/1.45 W. The fundamental RF power is 3/4 W, and HOM power 1/4 W at 2K. (Assuming 15MV/m, Q= 3×10^9, 10% HOM power at 2K.)

Infrastructure is being set up at DESY. An industrial building is being devoted to the Tesla activity. The final processing and preparation of the industrially produced cavities will be carried out with state of the art facilities. These include or make use of: cleanrooms (classes 100 and 10,000), chemical treatment and high purity water rinse; 1200C vacuum oven for improvement of the RRR and thermal conductivity of the Nb cavities; and vertical dewar high peak power (HPP) RF processing, gradient, and Q measurements of the bare cavitiy units. Finally the helium containment shell is attached and the couplers and tuners are mounted, and followed by a test of individual "dressed" cavities. This operation is performed in a horizontal test cryostat prior to the final assembly in the 8 cavity cryomodule. As experience is learned at obtaining reliable high gradient cavity performance, simplification and cost savings in the processing steps will be attempted. The initial infrastructure will be as complete as possible in order to assure the highest probability of success.

It should be pointed out that the push to high gradients in multi-cell 1.3 GHz cavities is already underway at Cornell[4] and CEBAF continues to gain experience at 1.5 GHz.

The four cryomodules, consisting of 32 cavities and 4 sets of focusing–steering elements at the cryo interfaces will be configured as a test string for beam as well as engineering systems tests. Two types of injectors, both operating at $\approx 8mA$ are under consideration. The first would be a low bunch charge injector with a conventional thermonic gun, chopper and buncher section operating at 300kV into one

of the standard 1m sc cavities. The injector beam energy would be 14 MeV. The second injector under consideration would provide the 5×10^{10} bunch charge at 1 microsec spacing. An effort is underway to evaluate this gun; a high gradient rf photocathode gun looks most promising. A thermionic gun will also be evaluated. Simulations with asymetric emittances will be carried out to see what emittance looks possible. For the TTF tests bunch charge is important but design emittance is not as important. A warm section between the injector and the standard cryomodules will provide an optics match and beam analysis area. Similarly there will be an analysis area after the four modules. Provision will be made to allow for beam offset of 1 cm or more in order to produce large transverse wakes.

Test Program for the TTF

Cavity Performance–Transfer full RF pulse power to beam at full pulse length. Attempt in-situ HPP processing of cavities in the string at the 1 MW level and experiment with different failure modes which might effect the cavity operation (e.g., vacuum failure).

Measure Q vs gradient with and without beam. As this will need to be done calorimetrically in the string, only low Q's below 10^9 will be detectable. Most Q measurements will come from the test cryostat data.

Measure the higher order mode power produced by the 5×10^{10} bunches and determine the fraction removed by: the HOM couplers, the microwave absorbers at the interfaces of the cryomodules (every 8 cavties), and that dissipated at 2 K in the helium. Look for transverse mode excitation by the beam as a function of beam position and see if one can measure cavity alignment by looking for a minimun in the transverse exicitation. Measure dark current, radiation patterns and energy spectrum without beam and determine the extent of captured dark current transported through the string.

RF System and Control–Develop a cavity, coupler tune up proceedure to control voltage, phase and coupling of the 16 cavities connected to one RF modulator. Measure the gradient and phase in each cavity as a function of time. Develope a quench, spark detection, protection system that allows for sufficient RF uptime. Develop cavity tune adjustment, radiation pressure compensation, and beam loading compensation. Look for and learn to control microphonics, coupler vibration, and radiation pressure effects that result in cavity tune , voltage or phase variations.

Beam Measurements–Measure the beam energy,energy spread, and energy and positional stability bunch by bunch as a function of bunch intensity, RF phase, bunch length, etc. Look for wake field and transverse mode excitation, and perform measurements of emittance blow up of off axis beams. (Many of the wake field measurements will require high intensity bunches.)

Cryogenics–Measure heat leak with and without RF and beam to determine static, RF fundamental, and HOM losses. Be able to detect cavities with low Q (10^9) and detect quenches. Measure operating performance as a function of temperature and measure the temperature profile for each cell and coupler on at least one cavity (this might be best done in the horizontal single cavity test cryostat.

Alignment and Vibration–Measure the cryomodule alignment stability and reproducibility during cool-down/warm-up. Measure the vibrational properties and transfer function of the cavities and quadrupoles.

Operation–Develop tune up procedure, practice beam alignment and focusing, simulate fault conditions for the subsystems. Check the beam position system operation and stability, and try to make precission measurements of beam transmittion (or losses).

Schedule for the TTF

- two model cavities to test infrastructure - summer 93
- infrastructure: cleanroom, chemistry, furnace - fall 93
- cryosystem & HPP rf - winter 93
- treatment/test of first 8 cavities - spring/summer 94
- assembly 1st cryomodule - fall 94
- install and operate 1st cryomodule winter - 94/95
- beam test 1st cryomodule - summer/fall 95
- cavities for 2nd -4th modules - mid 95/mid 96
- install modules 2-4 in test string - 96/97
- beam tests complete TTF - 97

References

[1] The TESLA R&D effort (TESLA=TeV electron superconducting linear accelerator) is being carried out by an international collaboration led by DESY. A number of institutions have joined this collaboration and include IHEP Beijing, Tech Univ Berlin, CEN Saclay, CERN, Cornell, TH Darmstadt, DESY,Fermilab, Univ. Frankfurt, INFN Frascati-Milan, Univ. Karlsruhe, KEK, LAL Orsay, IPN Orsay, SETF Finland, Univ. Wuppertal.

[2] M. Tigner, SLAC Beamline, Fall 1992, Vol. 22, #3.

[3] D. Trines *et al*, Proceedings, International Accelerator Conference, Hamburg, July 1992.

[4] J. Kirchgessner *et al*, this conference.

TESLA Input Coupler Development

M. Champion, D. Peterson, T. Peterson, C. Reid, M. Ruschman
Fermi National Accelerator Laboratory*
P. O. Box 500, Batavia, Illinois 60510

Abstract

The TeV Superconducting Linear Accelerator (TESLA) requires a RF input coupler capable of delivering 208 kW of 1.3 GHz power to a 9-cell Niobium cavity. Various electrical, mechanical, and cryogenic constraints present challenges in the design of such a coupler. Two parallel input coupler development programs are in progress at Fermilab and at DESY [1]. The Fermilab TESLA input coupler design and status is reported.

I. INTRODUCTION

The TESLA machine [2] is a next generation electron-positron collider based on two superconducting linear accelerators, each having a length of 10 km. Center of mass energies of greater than 500 GeV are planned, which will require accelerating gradients of 25 MV/m. Nine-cell superconducting Niobium cavities operating in the π-mode at 1.3 GHz will be used for acceleration. Each cryomodule will contain eight cavities with one input coupler and two higher order mode couplers per cavity. The coaxial input coupler (Fig. 1) is mounted to the beam tube adjacent to the end cell of the cavity and is capacitively coupled to the cavity. RF power for two cryomodules (16 cavities) will be provided by a single 4.5 MW klystron.

* Operated by Universities Research Association, Inc., under contract with the United States Department of Energy.

II. INPUT COUPLER DESIGN

A. Electrical

A critical component of the TESLA machine is the input coupler, which during normal operation must transport 208 kW of 1.3 GHz RF power to a 9-cell Niobium cavity. The pulse length is 1.33 ms with 0.53 ms filling time and 0.8 ms beam-on time. The repetition rate is 10 Hz, hence the average power through the coupler is nominally 2.8 kW. Additionally, it is desirable that the coupler handle power levels up to 1 MW (at reduced pulse lengths and repetition rates) so that *in situ* high peak power processing of field emission sites may be performed. At power levels of 1 MW, field strengths at the inner conductor near the cavity (outer

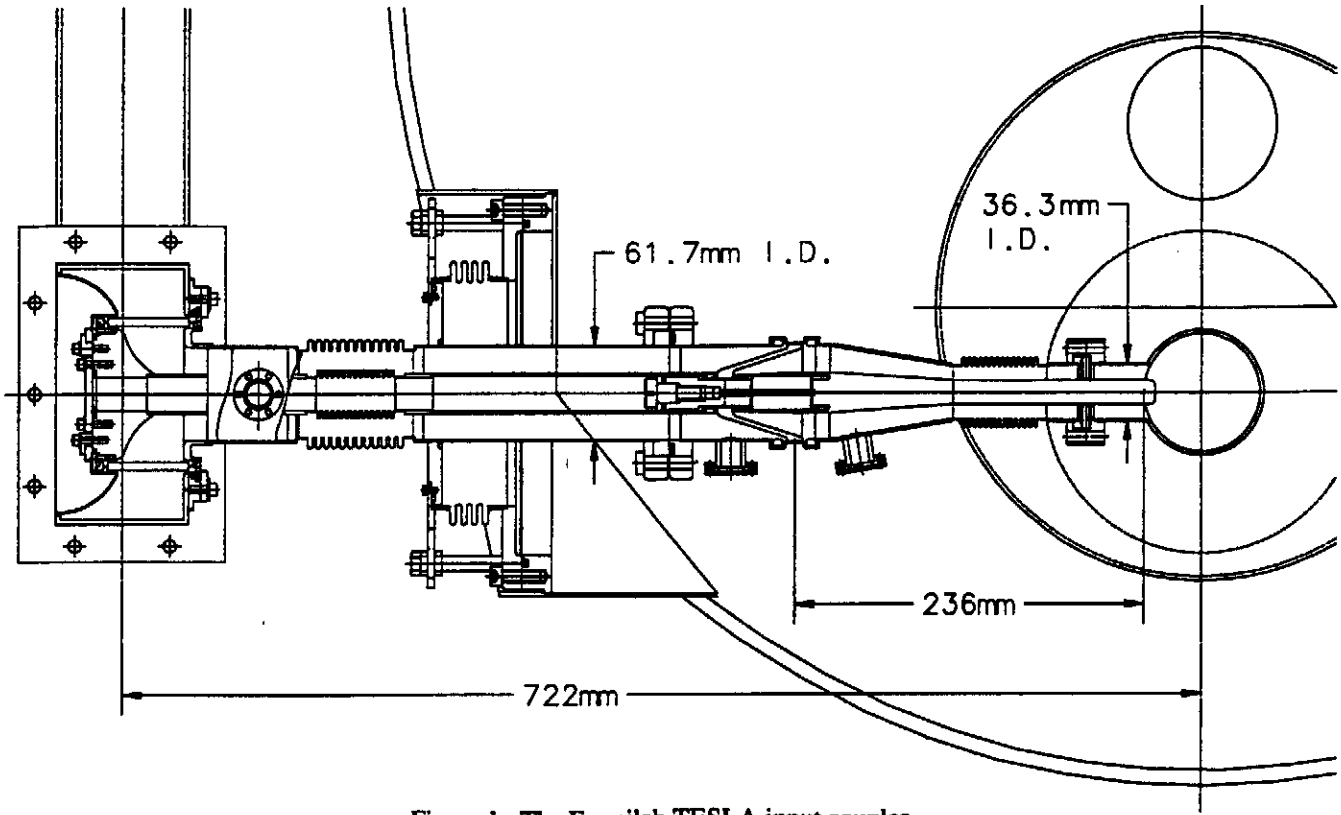

Figure 1. The Fermilab TESLA input coupler.

conductor diameter is 36 mm) will reach 3.04 MV/m for the case of total reflection as the cavity begins to fill with energy. The external Q of the coupler is to be 3e6, adjustable over the range 1e6 to 9e6. The variable coupling is required due to variations in the cavities, couplers, and RF distribution system. The input coupler should be impedance matched for a return loss of better than 20 dB (1 % power reflection).

B. Mechanical

The requirement of variable coupling is met by the use of bellows on the inner and outer conductors of the coaxial input coupler as shown in Fig. 1. The inner and outer conductors move together toward or away from the beam tube by adjusting bolts outside the cryomodule. A range of motion of up to 25 mm is possible, which is adequate for the required range of external Q.

During cool down the eight cavities shrink toward one fixed point at the center of the cryomodule. The input couplers must accommodate this shrinkage, which is 15 mm worst case. Since the waveguide end of the input coupler is fixed, the coupler must be flexible so that the cavity end of the coupler can move with the cavity. This flexibility is achieved via the inner and outer conductor bellows. There is a pivot point outside of the cryomodule about which the coupler can rotate as the cavities shrink. The coupler will be mounted at room temperature so that the center conductor is off center at the beam tube. As the system shrinks during cool down, the center conductor will pivot into a position concentric to the outer conductor. Coupling adjustment will follow the cool down.

In opposition to the requirement for flexibility, there is a need to avoid mechanical vibration of the input coupler, which could lead to difficulties in controlling the amplitude and phase of the RF drive to the cavity. After coupling adjustment is complete, bolts will be tightened to secure the coupler at the cryomodule penetration.

The cold RF window must stay with the cavity once the cavity has been assembled in a clean room. Hence, the portion of the input coupler which extends out of the cryomodule must be removable. This is accomplished with an outer conductor flange joint sealed with a Helicoflex metal seal and an inner conductor joint fastened with a screw.

C. Cryogenic

The input coupler connects room temperature WR650 waveguide to a cavity at 1.8 K, hence minimum heat leak is necessary. This is achieved by using copper plated thin-wall stainless steel coaxial transmission line. Thermal calculations have been performed and indicate a 70 K heat load of 5.8 W and a 4 K heat load of 0.4 W.

D. Vacuum/Cleanliness

Two alumina ceramic RF windows will act as vacuum barriers and ensure the cleanliness of the cavity. A cylindrical window is utilized in the waveguide to coaxial transition, while a conical window is installed at the 70 K intercept in the 62 cm diameter coaxial line. Ports for pumping and instrumentation of the region between the two windows are included near the waveguide.

III. COMPONENT DEVELOPMENT

A. Conical Ceramic

The conical ceramic window is the first level of protection of the cavity vacuum space. The conical shape was conceived of as a good candidate for a broad band impedance-matched window. The angle formed by the cone with respect to the axis of the coaxial line was chosen to be 18.2 degrees, which is the result of setting the angle of incidence equal to the Brewster angle for the vacuum to ceramic interface. The depth of penetration of the ceramic into both the inner and outer conductors was chosen to reduce the field strengths at the braze joints to approximately 50 % of their nominal values at the surfaces of both conductors. Two possibilities were examined for obtaining a good impedance match. One technique is to taper the ceramic thickness so that it is thinner near the inner conductor. The other method is to taper the inner or outer conductors. The tapered ceramic was rejected in order to simplify the ceramic, and because it is easier to machine metal to a new shape than to modify the ceramic. We chose to taper the inner conductor due to ease of fabrication. The thickness of the ceramic in the conical region is 3.2 mm. The Hewlett-Packard High Frequency Structure Simulator (HFSS) was used to model the ceramic. A return loss of 22 dB was achieved during simulation by iterating on the inner conductor taper.

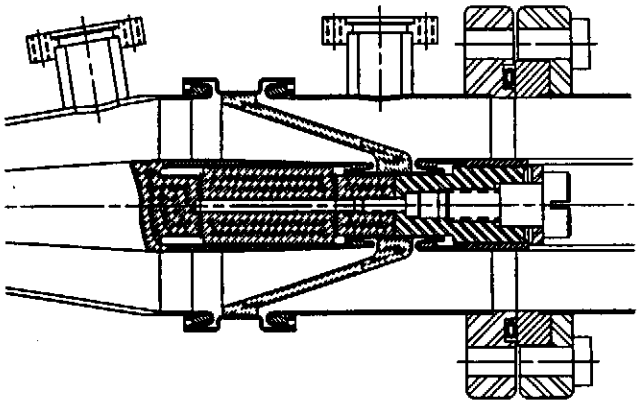

Figure 2. Detail of conical ceramic RF vacuum window.

Implementation of the design is shown in Figure 2. The ceramic is 99.5% Al_2O_3 from WESGO. The OFHC copper inner and outer conductor bands were brazed to the ceramic by Alberox. Initially, the inner conductor band contained a small plug of ceramic to prevent the band from shrinking away from the cone during the brazing cool down period. However, this plug caused cracking of the cone during brazing. The ceramic was coated with Titanium Nitride (TiN) by an evaporative

process at Fermilab. The conical shape requires several evaporations with various filaments in order to achieve a relatively uniform TiN thickness. The thickness goal was 10 nm on the ceramics coated to date. The inner conductors on each side of the ceramic were attached via electron beam welding at Fermilab. The outer conductors were attached via conventional TIG welding in an Helium/Argon atmosphere.

B. Bellows

The bellows used in the prototype input coupler are off-the-shelf units that have adapters resistance welded to each end. The thin wall (0.006") bellows are hydroformed and are rated for a range of travel of 25.4 mm. Copper plating of the outer conductor bellows along with the attached stainless steel tubing is achieved by using a special apparatus consisting of a tubular electrode which is inserted into the outer conductor and is sealed at the opening of the conductor. Plating solution enters the outer conductor through holes drilled in the electrode. The other end of the outer conductor is covered with a plate that has an exit port and attached tubing to carry away the plating solution. Hence, solution is continually circulated through the outer conductor during the plating process, and the exterior of the conductor remains free of plating.

C. Doorknob Transition

The "doorknob" transition is a waveguide to coaxial transition that incorporates a cylindrical knob as the impedance transforming device. This type of transition, when properly designed, has been shown to be capable of transmitting power up to the breakdown level of the coaxial line [3]. The Fermilab doorknob transition (Fig. 3) is complicated by the decision to incorporate a cylindrical ceramic window into the transition. Not only is the transition more difficult mechanically, but also the inclusion of the window tends to reduce the bandwidth of the transition to 1-2 percent. However, this complication makes for a compact and elegant impedance transformer and vacuum barrier.

The ceramic is 99.5 % Al_2O_3 from WESGO. Fermilab fabricated the OFHC copper and 304 SS rings which were brazed to the ceramic by Alberox. The ceramic is to be TiN coated on the vacuum side (inner surface). The waveguide side of the ceramic will be exposed to > 1 Atm dry air.

The addition of a window results in the use of a two-piece doorknob. The outer piece is welded to the waveguide, whereas the inner piece is welded to the ceramic window. The ceramic and inner knob are bolted into the waveguide assembly, so the ceramic may be replaced if necessary. C-seals are used as RF joints in the bolted assembly. The shape and size of the doorknob determines the impedance characteristics of the transition. These parameters have been determined by "cut and try techniques." The HFSS program has been used to model the design and help understand the field characteristics of the transition.

IV. CONCLUSION

A prototype of the coaxial portion has been constructed and tested at 805 MHz at power levels up to 1.7 MW [4]. The design needs to be optimized in terms of impedance match, cost, and assembly procedures. Testing at 1.3 GHz is expected in the coming months.

A low-power prototype of the doorknob transition has been constructed and tested. Impedance matching has been achieved over a 1-2 % bandwidth. A prototype high-power transition is under development and should be ready for testing by July, 1993.

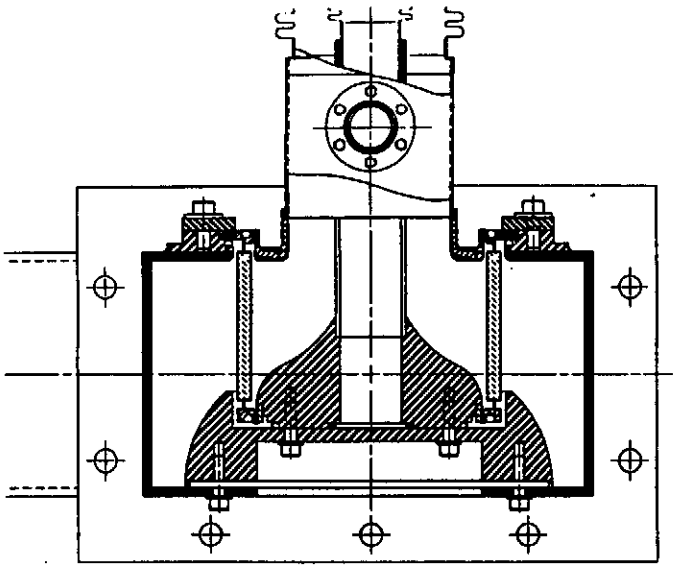

Figure 3. Detail of doorknob transition.

V. REFERENCES

[1] B. Dwersteg, M. Marx, D. Proch, "Conceptual Design of a RF Input Coupler for TESLA," DESY, 1992.

[2] *A Proposal to Construct and Test Prototype Superconducting RF Structures for Linear Colliders*, DESY, 1992.

[3] G. L. Ragan, ed., *Microwave Transmission Circuits*, Boston Technical Publishers, Inc., 1964.

[4] D. Sun, M. Champion, M. Gormley, Q. Kerns, K. Koepke, A. Moretti, "High Power Test of RF Window and Coaxial Line in Vacuum," Fermilab, these proceedings.

High Power Test of RF Window and Coaxial Line in Vacuum

D. Sun, M. Champion, M. Gormley, Q. Kerns, K. Koepke, A. Moretti
Fermi National Accelerator Laboratory*
P.O. Box 500, Batavia, Il 60510

Abstract

Primary rf input couplers for the superconducting accelerating cavities of the TESLA electron linear accelerator test to be performed at DESY, Hamburg, Germany are under development at both DESY and Fermilab. The input couplers consist of a WR650 waveguide to coaxial line transition with an integral ceramic window, a coaxial connection to the superconducting accelerating cavity with a second ceramic window located at the liquid nitrogen heat intercept location, and bellows on both sides of the cold window to allow for cavity motion during cooldown, coupling adjustments and easier assembly. To permit in situ high peak power processing of the TESLA superconducting accelerating cavities, the input couplers are designed to transmit nominally 1 ms long, 1 MW peak, 1.3 GHz rf pulses from the WR650 waveguide at room temperature to the cavities at 1.8 K. The coaxial part of the Fermilab TESLA input coupler design has been tested up to 1.7 MW using the prototype 805 MHz rf source located at the A0 service building of the Tevatron. The rf source, the testing system and the test results are described.

I. INTRODUCTION

TESLA [1] is a proposed 500 GeV center of mass energy e+e- linear collider utilizing superconducting rf accelerating cavities. An international effort under the direction of DESY is collaborating to assemble a TESLA test facility at DESY including an electron source, 40 m of superconducting accelerating cavities, cryostats, accelerating rf, beam diagnostics, and the infrastructure necessary to produce and test the superconducting cavities.

A TESLA accelerating module consists of a cryostat nominally 10 m long and contains 8 niobium accelerating cavities. Each accelerating cavity is nominally 1 m long and contains 9 contiguous niobium accelerating cells that are tuned to 1.3 GHz. Each 9 cell cavity is excited in the pi mode with a single input coupler.

Input couplers are under development at DESY [2] and Fermilab [3]. The Fermilab input coupler design is shown in Figure 1. The function of the input coupler is to transmit the rf energy from the klystron power distribution system, WR650 waveguide at room temperature, to the cavities at 1.8 K. The cylindrical ceramic window within the WR650 "doorknob" transition isolates the pressurized waveguide from the required high vacuum of the cold coaxial section. The conical ceramic window maintains the ultraclean environment required by the superconducting cavities during their assembly and testing. During normal operation, this window acts as backup to the warm window and prevents contamination of the entire accelerator in the event of a warm ceramic window failure.

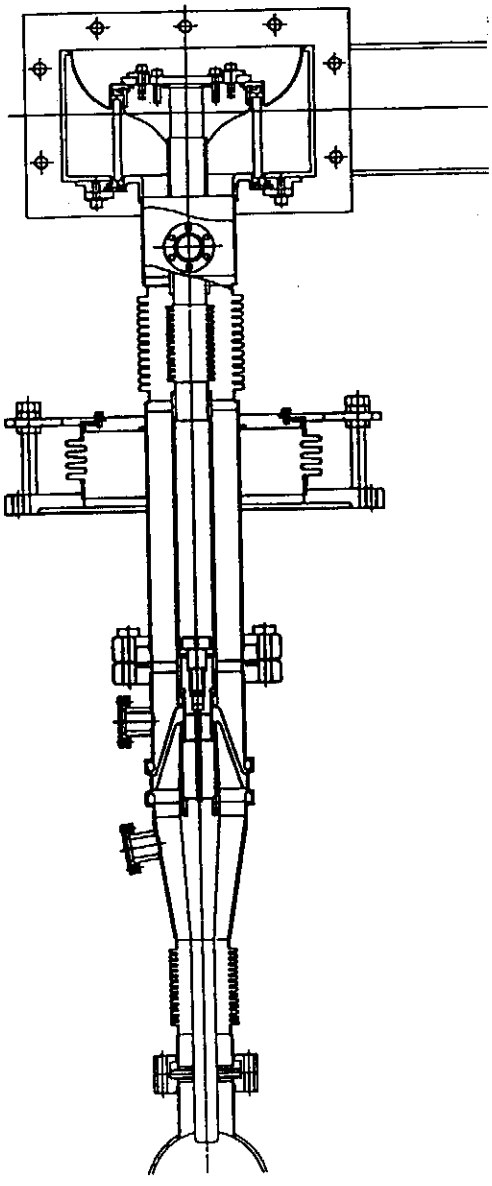

Figure 1. TESLA input coupler tested at A0.

*Operated by Universities Research Association under contract to the U.S. Department of Energy.

Normal operating conditions for the coupler during beam acceleration are a peak power of 200 kW, a nominal 2 ms pulse length and a pulse repetition rate of 10 Hz. An estimated 1 MW peak power with reduced pulse length and repetition rate to keep the average coupler power unchanged, is necessary if in situ high peak power conditioning of the cavities is planned. At this peak power level, the performance of the coupler, and in particular, the behavior of the ceramic windows and bellows, can no longer be reliably predicted, and at the very least, careful initial rf conditioning of the coupler is expected to be necessary before it functions reliably.

As an rf system at 1.3 GHz and at a peak power level above 1 MW is currently not available to us, we have used the operating spare klystron of the Fermilab linac upgrade [4] to test the coaxial part of the Fermilab TESLA input coupler. This source is located in the A0 service building of the Tevatron where it was previously used to rf condition the Fermilab Linac Upgrade accelerating cavities. The rf source produces 120 μs long, 12 MW peak power rf pulses at a frequency of 805 MHz. Except for multipactoring, the difference in operating frequency does not significantly affect the behavior of the coaxial part of the input coupler as it was designed to have a constant 50 ohm impedance throughout, and the conical ceramic window is "thin". The complete coupler, including the "doorknob" transition with its narrow band width, will be tested at a later date with a 1.3 GHz rf system under assembly at Fermilab.

II. GEOMETRY AND INSTRUMENTATION

The goals of the rf tests at A0 were to subject TESLA input coupler components to peak power levels at least equal to their 1 MW design level, to find the rf breakdown thresholds by raising, if necessary, the peak rf power above 1 MW , and to determine the locations and mechanisms of the rf breakdown. These goals necessitated a somewhat more elaborate test geometry than normally used to condition rf components.

The test equipment that has been added to the A0 rf system is depicted in Figure 2. The rf power enters and leaves the test equipment through the two WR975 to 3 1/8 inch coax couplers shown at the bottom of the figure. Not shown are the forward and backward directional couplers in the waveguide upstream of the test insertion to measure the rf power, and the waveguide ceramic windows contiguous to the WR975 couplers to allow high vacuum in the test device. Two standard 3 1/8 inch rigid coax sections, each 12 inches long, and two rigid 3 1/8 inch coaxial elbows complete the rf circuit. The test geometry is physically symmetric relative to the test device. The coaxial part of the TESLA input coupler tested has an outer coaxial diameter between 4 cm to 6 cm. Therefore,

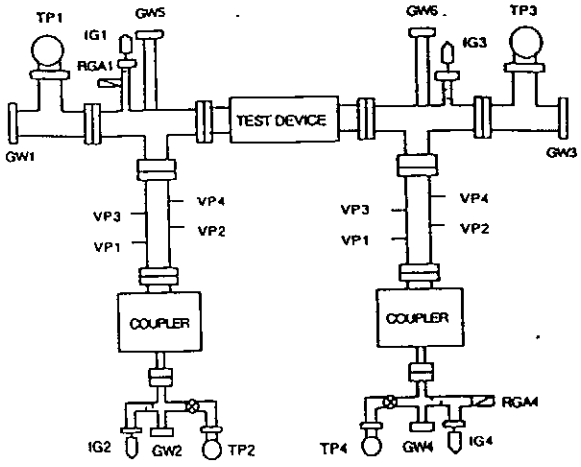

A0 TEST SETUP

TP: TURBO PUMP
IG: ION GAUGE
RGA: RESIDUAL GAS ANALYZER
GW: GLASS WINDOW
VP: VOLTAGE PROBE

Figure 2. Test geometry used to test the input coupler.

conical transitions were used to match the inner and outer coax conductors to the 3 1/8 inch rigid coax on either side of the test device. The rf insertion is approximately matched and most of the power is absorbed by an rf load located downstream of the test circuit.

Four turbo pumps were used to evacuate the test volume. Four ion gauges and a residual gas analyzer were used to monitor the vacuum during pumpdown and during the rf testing. Six glass windows, two in line with the test device (GW1 and GW3) and their associated photomultipliers were used to monitor the light output within the test volume. Two additional windows, one glass with a photomultiplier and one KBr window for an infrared monitor, were mounted on either side and close to the cold TESLA window to monitor this critical area. Finally, 8 rf voltage taps spaced 1/8 wavelength apart, 4 upstream and 4 downstream of the test device, were available to locate a breakdown region in the event that the breakdown reflected a measurable amount of rf power.

The controls of the A0 rf system contain 8 triggerable data recording channels that were intended to record transient signals during klystron modulator performance checks or fault diagnosis. Each data channel consists of a digitizer connected to a 120 μs circular buffer with a 1 μs time resolution. These channels were available for transient analysis. In addition, a single data

point per channel was recorded 4 times per minute and stored in a Sun Work Station to maintain a slow time record of the test over many days.

III. PROCEDURE

During the test, the rf pulse length and pulse repetition rate were maintained at 120 μs and 15 Hz, the maximum available from the A0 rf system. The average vacuum at the start of the test was 2.8 10-7 torr. The peak rf power was increased in steps; the amplitude increase per step was determined by the vacuum pressure which was arbitrarily maintained below 2.0 10-6 torr. The vacuum pressure was allowed to recover at constant rf power until it reached a pressure of 4.0 10-7 torr at which point the rf power was again increased. The power threshold at which the vacuum first responded to the rf was 3.6 kW.

The photomultipliers were calibrated by measuring their outputs when located at the same position. Their outputs indicate relative light intensities as a function of rf power, time, and location. The photomultiplier outputs were continuously observed during the coupler conditioning but were not used to determine the rate at which the rf power was increased.

The temperature of the conical ceramic window was monitored with an infrared detector looking directly at the ceramic, and with two thermocouples located on the outer coax conductor near the location where the ceramic was attached with a braze joint. These thermometers were monitored to prevent damage to the ceramic due to thermal stress, and to record the heating rate of the ceramic as a function of rf power through the ceramic window.

IV. RESULTS

Testing has been in progress for one week. The coupler was conditioned to a 1.4 MW peak power level within three days. This time could have been reduced to two days with an automatic conditioning system as the system was operated at a constant reduced power level (20kW and 100 kW) while unattended overnight. Since this initial conditioning, the coupler has operated without interruption for 40 hours at a peak power level of 230 kW, for 16 hours at 1 MW, and 1 hour at 1.7 MW.

During conditioning, the klystron shut off twice due to a klystron window spark and/or high reflected rf power. The first trip occurred at 1.3 MW. The cause of this trip has not been established. The second trip occurred at 1.44 MW and was caused by a spark downstream of the conical window, perhaps in the 4 cm region of the coupler or in the 3 1/8 inch transition. This spark was isolated through high light output at GW3 and GW4, the photomultipliers mounted downstream of the conical window, by low light output from the photomultiplier mounted by the conical window, and by the high vacuum pressure downstream of the conical window. Since then, several more sparks have occurred, apparently in the downstream region, all at or above a peak power level of 1.4 MW.

Steady light related to the rf power has been observed by the photomultiplier located at GW1, that looks at the upstream part of the coupler as far as the conical window, by the photomultiplier located immediately downstream of the conical window, and by the photomultiplier located on the downstream waveguide transition (GW4). The light at GW4 can be conditioned away, reappearing only if the rf is turned to a lower level for an extended time and then returned to its higher original level. The light on either side of the conical window occurs at specific power levels, increasing and decreasing as the power is continuously raised, and up to now has not been completely conditioned away.

V. CONCLUSIONS

The conical part of the tested TESLA input coupler appears to satisfy the normal peak power operating condition of 200 kW. After conditioning, no light is seen below a peak power of 230 kW. Effort continues to understand and eliminate the light still present. A possibility is to locate the conical window at a voltage minimum to reduce the voltage at the window during mismatched operation.

Operation at a peak power level of 1 MW for in situ high peak power conditioning of the cavities is still not certain. Some light during conditioning is acceptable as the conditioning time is short. However, the location of the observed sparks needs to be determined and the cause corrected.

VI. REFERENCES

[1] *A Proposal to Construct and Test Prototype Superconducting R. F. Structures for Linear Colliders,* DESY, April 1992

[2] B. Dwersteg, M. Marx, D. Proch, "Conceptional Design of a RF Input Coupler for TESLA", DESY 1992

[3] M. Champion, D. Peterson, T. Peterson, C. Reid, "Tesla Input Coupler Development", these proceedings

[4] H. Pfeffer, et al, "Solid State 24 MW Modulator for Fermilab's 400 MeV Linac", Twentieth Power Modulator Conference, Myrtle Beach, South Carolina, June 1992

A new surface treatment for niobium superconducting cavities

B. Bonin, C. Henriot, C. Antoine, B. Coadou, F. Koechlin, J.P. Rodriguez, Groupe d'Etudes des Cavités Supraconductrices
DAPNIA-SEA, CE Saclay, F-91191 Gif/Yvette, France
E. Lemaître, P. Greiner, Laboratoire Moderne de Soudage
DTA-CEREM-DTM-STA-LMS, CE Saclay, F-91191 Gif/Yvette, France

Abstract

A condition necessary for the successful performance of superconducting cavities is the cleanliness of their inner surface. The firing of niobium cavities under vacuum at very high temperature is known to be a particularly effective method for cleaning the surface and for suppressing electron field emission. However, this process is inconvenient and expensive, if it is done in the "usual way", ie in a high vacuum furnace. We propose an alternative technique for cavity firing, using local heating in an electron beam or laser welding facility. This treatment is easy, and can readily be integrated in the usual process of cavity production. Initial tests at Saclay have given very promising results.

I. INTRODUCTION

The cleanliness of the inner surface of superconducting cavities is an indispensable condition for the successful performance of these accelerating structures. The firing of niobium cavities under vacuum at very high temperature is in wide favor in many laboratories for at least two reasons : i) when used in association with solid state gettering (e.g. titanification or yttrification [1]), it permits a purification and a homogenization of the material, with a subsequent improvement of its thermal conductivity, and a better stabilization of the cavity against quenches; ii) this treatment seems to inhibit the activity of the microscopic sites where electron field emission takes place. The field emission threshold which limits the accelerating gradient available in the cavity is then pushed to higher levels.

However, firing is usually done in a high vacuum furnace, which makes the process inconvenient and expensive. There is also a very serious risk of recontamination of the cavity surface during the furnace venting, since the cavity is necessarily open during treatment. The benefits of the bulk purification of the material are then kept, but the protection of the cavity against field emission may be lost after the treatment. Firing of niobium cavities in a high vacuum furnace is thus difficult to integrate in an industrial process of cavity production.

We have explored an alternative technique, which employs local heating in an electron beam welding facility. The interst of the method lies mainly in its simplicity and its rapidity. The local character of the heating may also present some advantages : for instance, the cavity flanges can be spared during the treatment. This alleviates the need for refractory flanges, and opens up the interesting possibility of firing *closed* cavities.

II. EXPERIMENT

All the firing experiments were done in the EB welding machine of LMS, at Saclay. Its TECHMETA electron gun delivers an electron beam of controllable energy, intensity and focusing. The electron beam pencil can be moved and vibrated across the sample surface by means of suitable deflecting electrodes. The vacuum in the vessel is no better than 10^{-3} Pa.

The first firing tests were made on 2mm thick niobium sheet samples. The sample temperature during firing was measured by means of a bichromatic optical pyrometer viewing the sample through a window in the EB welding machine. The accuracy of the measurement was on the order of ± 100°.

In all practical cases, the electron beam dwell time on one given point of the surface was long as compared to the characteristic time of heat diffusion across the niobium sheet. For this reason, we believe that the temperature was identical on both sides of the sheet.

The first tests showed that any chosen temperature between 1000° and 2000° C could be reached and maintained with excellent stability, by a suitable choice of the following parameters : electron energy, beam size, beam intensity and displacement speed.

The fired samples showed a considerable recrystallization: starting from an initial grain size of 50–70 μm, the final grain size was as large as 1 cm for the hottest and longest runs. The initial purity of the Nb samples was RRR=200. No degradation of RRR was observed for the shortest runs (15 sec), but a significant loss of purity (RRR=50) resulted from the long firings (15 min), even at very high temperature. This is attributable to the fact that residual gaseous species present in the vacuum enter readily as interstitials in the niobium lattice at high temperature [2,3]. The important degradation observed can then be ascribed to the poor vacuum in the welding machine.

These considerations led us to protect the niobium before and during firing, by means of a titanium vapor layer deposited on the sample surface by sublimation of a joule—heated titanium filament. Contamination from the residual gases is then confined to the outside titanium layer, and no longer affects the bulk niobium. New RRR measurements after this treatment showed no purity degradation, thus confirming the success of this protection method. In the present experiment, the Ti layer could be deposited only on one side of the Nb sheet sample. In this case, there is probably competition between a pollution of the material from the unprotected side, and a purification from the titanified one. A real purification of the bulk material

could be expected from a more careful titanification, covering both sides of the sample.

As compared to the titanification in general use for the firing of niobium cavities in high vacuum furnaces [1], the above-mentioned method has the advantage that the Ti filament and the niobium sample to be treated are heated separately to (eventually) different temperatures. This gives an appreciable control of the sublimation rate and of the thickness of the Ti layer on the sample surface during firing. This nice feature, which allows the deposition of the titanium layer *before* the firing, should improve the efficiency of the titanification by suppressing the risk of pollution during the passage through the dangerous temperature zone where the niobium is already hot enough for the impurities to enter, and is still unprotected by the titanium sublimation.

In order to assess the validity of the technique for the practical treatment of superconducting cavities, a single cell, 1.5 GHz niobium cavity was heated in the EB machine, with the following particular features :

1) The cavity was mounted on a horizontal mandrel and rotated in front of the fixed electron beam ;

2) The cavity was titanified from outside by sublimation of a joule-heated titanium filament parallel to the cavity axis ;

3) The cavity -already equipped with its antennas- had been sealed under static vacuum before firing. The motivation for this sealing was to protect the cavity against pollution by the (poor) residual vacuum during firing, and against any ulterior contamination by dust particles or by chemical species after firing. The cavity was not reopened after the treatment, and was directly tested in a vertical cryostat, still under the same static vacuum ;

4) All points of the cavity surface were maintained at 1850° C during 1 minute. After the heat treatment, the cavity surface showed the same considerable recrystallization as was observed on sheet samples. No noticeable deformation of the cavity shape could be detected.

This cavity showed excellent RF performance, giving an accelerating gradient of 19 MV/m and a residual Q value above 10^{10} without any electron emission. Although we consider this result very encouraging, it must be noted that this gradient and Q value had previously been obtained with this same cavity after a standard chemical treatment and mounting. Hence, we cannot claim an improvement of the cavity performance due to the heat treatment.

Clearly, the curative virtues of the treatment are still to be demonstrated, but there is some hope that this kind of firing might replace the delicate chemical etching, rinsing and clean-room drying that represent the "state of the art" for superconducting accelerating cavities.

VI. CONCLUSION

We have shown that an electron beam heat treatment of niobium superconducting cavities is an interesting possibility, probably superior to the usual high vacuum furnace heat treatment. Suitable electron beams are already available in industry in EB welding machines, whereas high vacuum furnaces are still laboratory objects. The poor vacuum of our EB welder obliged us to contrive complicated arrangements to avoid the pollution of the niobium by residual gases. However, EB welding facilities with improved vacuum (10^{-5} Pa) are available. In such devices, a high vacuum level during treatment would certainly be easier to achieve than in furnaces, because there are no screens and because the only hot surface is the desired one. The potential cleanliness of this kind of heat treatment is thus excellent. The local heating of the surface opens rich perspectives, which have not yet been explored. Experiments are under way at Saclay to determine the benefits that can be obtained from such a treatment, from the points of view of curing field emission and purifying niobium. The parameters of the treatment (temperature, duration) remain to be determined.

The help of the "Groupe d'Etudes des Cavités Supraconductrices" for testing the cavity is gratefully acknowledged.

VII. REFERENCES

[1] H. Padamsee et al., IEEE T. Mag 21 1007 (1985)
[2] M. Hörmann, J. Less Comm. Metals 139 1 (1988)
[3] K.K. Schulze, J. Metals, May 1981 p.33

Progress on RF superconductivity at Saclay

Groupe d'Etudes des Cavités Supraconductrices* DAPNIA-SEA, CE Saclay, F-91191 Gif/Yvette, France
and Institut de Physique Nucléaire** Université de Paris Sud, F-91400 Orsay, France

Abstract

We report substantial progress in R&D on superconducting accelerating cavities at Saclay.

I. INTRODUCTION

The Saclay program of R&D on RF superconductivity has been actively pursued, aiming at applications in the frame of the TESLA and "European Electron Accelerator for Nuclear Physics" projects. The most important issues of this research are the quest for high accelerating gradients and reduced RF dissipation.

II. HIGH GRADIENTS

The gradients available in superconducting cavities are now limited mainly by field emission. This phenomenon has been studied on samples, in both DC and RF regimes, with specific facilities. We have confirmed that the electron emission in cavities is mainly due to micron sized dust particles. Selective contamination experiments showed that metallic particles behave as especially strong emitters. Greater care in cavity cleaning and mounting have in fact resulted in an improvement in cavity performance : accelerating gradients as high as 18 — 20 MV/m can now be reliably achieved in 1.5 GHz single cell cavities (Fig.1).

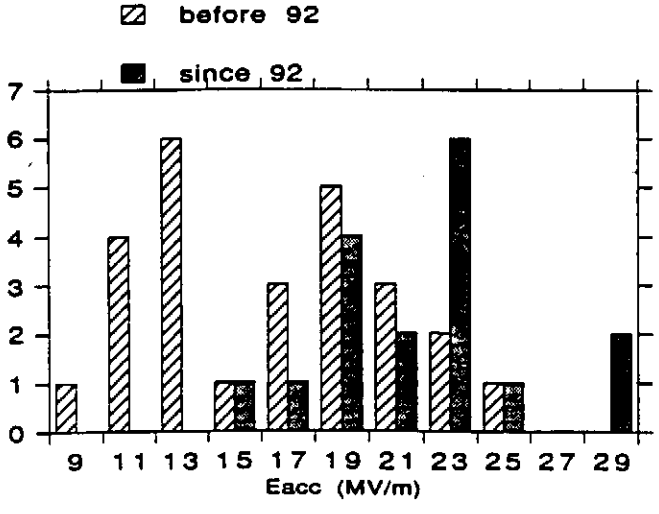

Figure 1 A large number of single cell Nb cavities at 1.5 GHz has now been tested at Saclay by the "Groupe d'Etudes des Cavités Supraconductrices". The corresponding systematics are summarized in Fig.1. It can be seen that the latest tests correspond to results significantly better than the older ones. The improvement is thought to be due to improved cleanliness during cavity treatment and mounting.

One cavity of this type, tested in the same laboratory, has reached an accelerating gradient of 28 MV/m (Fig.2) after a particularly careful surface treatment involving firing and titanification at 1300° C during 16 hours in a vacuum furnace, followed by chemical polishing, rinsing and drying in a recently developed automated facility [1].

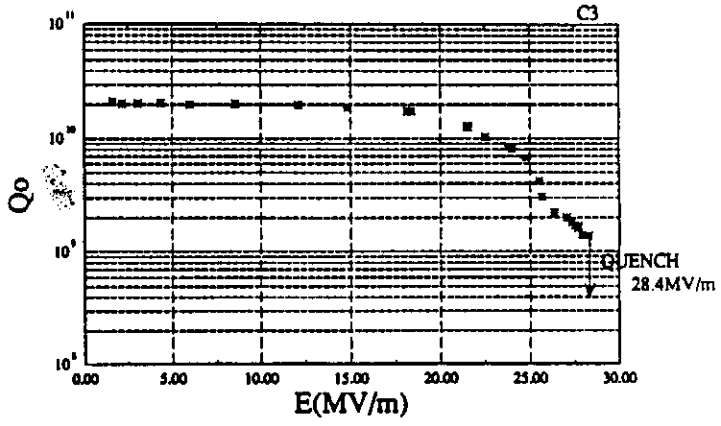

Figure 2 Q value vs accelerating gradient for the "high gradient" cavity

III. LOW DISSIPATION

The residual surface resistance routinely obtained in our Nb cavities is 15 nΩ at 1.5 GHz. The origin of the associated dissipation is now understood as the sum of the contribution due to trapping of the residual magnetic flux during cooldown, plus a new one due to the polycrystalline nature of the niobium used for making the cavities. Both contributions have been studied theoretically and experimentally [2]. This work opens the perspective of improved Q values for superconducting cavities.

A Q value of 5.10^{10}, corresponding to a residual surface resistance of 4 nΩ, has actually been reached recently with a 1-cell niobium accelerating cavity at 1.5 GHz (Figs 3,4). This is probably the best value ever obtained on an accelerating cavity in the GHz frequency range. The main reasons for this success are improved magnetic shielding and reduced RF losses at the ends of the cutoff tubes. The use of high purity niobium (RRR 320) may also have played a favourable role. We will now try to demonstrate the reproducibility of this result, and its validity in a real accelerator environment.

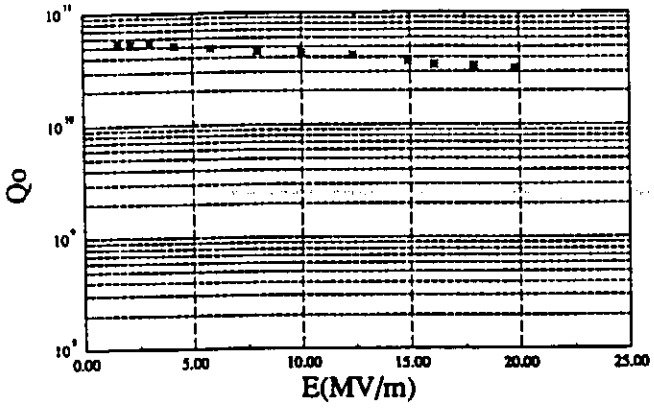

Figure 3 Q value vs accelerating gradient for the "low dissipation" cavity

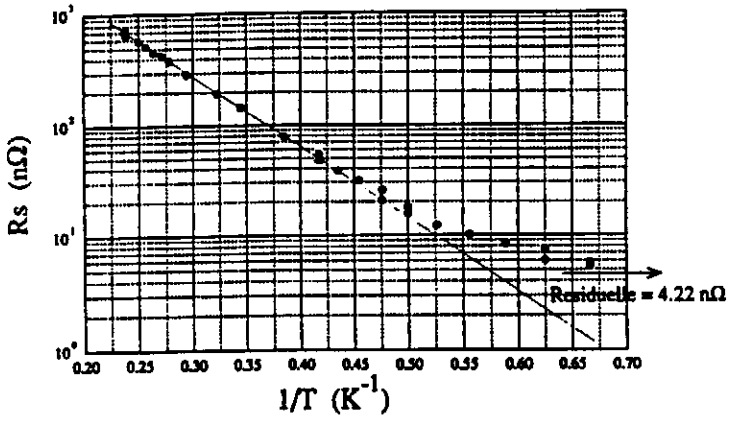

Figure 4 Surface resistance vs inverse temperature for the "low dissipation" cavity

IV. THIN SUPERCONDUCTING FILMS

Efforts have also been continued to develop the thin film coating technology at Saclay [3]. A sample of NbTiN film, deposited on copper substrate by magnetron sputtering, reached a RF field level of 35 mT and exhibited a low residual surface resistance (40 nΩ at 4 GHz), with a very small BCS resistance and an unusually small dependence of Rs vs RF field. If this result can be reproduced in a full scale accelerating cavity, the "thin film way" will certainly regain some credibility for the construction of superconducting structures.

V. PROGRESS ON THE ACCELERATOR MACSE

A continuous electron beam of 100 μA was accelerated in the MACSE prototype [4], with excellent stability, emittance and energy resolution (ΔE = 7 keV at E = 26 MeV). A distributed RF power scheme (one klystron for 4 cavities) was applied successfully, without energy spread degradation. Pulsed RF processing at moderate power (5 kW) suppressed e^- loading due to field emission in the MACSE cavities. The accelerating gradient was then limited by quench at an average value of 12 MV/m. A gradient as high as 18 MV/m was reached in one cavity. This is the first time that such a gradient is obtained with a superconducting cavity in an electron accelerator.

VI. CONCLUSION

These encouraging results confirm that superconducting cavities are still far from their limits and that the associated technology can make important progress, toward the construction of future large accelerators.

VII. REFERENCES

[1] C.Z. Antoine et al., Proc. 3rd European Part. Acc. Conf., Berlin (1992) 1319

[2] C. Vallet et al., Proc. 3rd European Part. Acc. Conf., Berlin (1992) 1295

[3] P. Bosland et al., Proc. 3rd European Part. Acc. Conf., Berlin (1992) 1316

[4] J.M. Cavedon et al., Proc. 3rd European Part. Acc. Conf., Berlin (1992) 52

* C. Antoine, B. Aune, M. Bolore, B. Bonin, P. Bosland, Y. Boudigou, J. Bourbonneux, M. Boussoukaya, S. Cantacuzino, J.P. Charrier, S. Chel, B. Coadou, A. Curtoni, B. Daillant, B. Delomez, M. Desmons, J. Gastebois, J. Gobin, J. Gratadour, B. Groux, X. Hanus, C. Henriot, M. Jablonka, M. Jimenez, J.M. Joly, G. Jouve, M. Juillard, E. Klein, F. Koechlin, C. Magne, B. Mahut, J. Martignac, A. Mosnier, R. Noer, J. Novo, B. Phung Ngoc, J.P. Poupeau, J.P. Rodriguez, D. Roudier, H. Safa, J. Tan, C. Vallet, A. Zeitoun.

** M. Caruette, M. Fouaidy, T. Junquera

A Generalized Method for Calculating Wake Potentials

Olivier Napoly*, Yong H. Chin† and Bruno Zotter‡

* DAPNIA-SEA, CE Saclay, F-91191 Gif/Yvette, France

† Lawrence Berkeley Laboratory, 1 Cyclotron Road, Berkeley, CA 94270, USA

‡ CERN, SL/AP, CH-1211 Geneva, Switzerland

Abstract

We describe a generalized method to compute wake potentials created in axisymmetric structures. It relies on expressing the wake potentials, of any multipole order, as integrals over the e.m. fields along an arbitrary one-dimensional contour spanning the structure longitudinally. For perfectly conducting structures, the integration along the axis can then be replaced by choosing a contour beginning and ending on the beam tubes. Thus it generalizes the former method of calculating the wake potentials by integrating along a straight line at the beam tube radius. Its usefulness is illustrated with the computer code ABCI which permits calculation of wake potentials in structures extending to the inside of the beam tube radius, or having unequal beam tube radii at the two sides.

I. INTRODUCTION

The determination of the wake potentials and impedances created by metallic structures surrounding the beam trajectory is an important issue in the design of accelerators. In most practical cases, the wake fields must be calculated with computer codes. For cavity-like structures symmetric about the beam axis, using the known radial dependence of the monopolar (m=0) longitudinal and dipolar (m=1) transverse potentials, the integration of the wake fields can be performed along a straight line parallel to the axis at the beam tube radius [1]. For perfectly conducting walls, the boundary conditions ensure that the integral along the beam tube vanishes for the tangential (longitudinal or azimuthal) components of the wake potential. This leaves the integral across the cavity gap as the only contribution to the wake potentials. This simplification is essential for computer calculations, in particular for long structures and short bunches requiring small mesh size and where long beam tubes would require excessive computer memory and cpu time. However, this technique does not work when the two beam tubes have unequal radii, or when part of the cavity extends to a smaller radius. If it is the case, for instance for tapers, steps, collimators or cavities with small aperture irises, the only alternative is to integrate along a straight line at an allowable radius, and with beam tubes as long as possible. Usually one must also subtract the wake potential of the beam tubes without structure ("numerical noise") which is different from zero due to the discretization of the geometry.

In this paper, we generalize the above straight-line integration method, by showing that the longitudinal and transverse wake potentials, at all orders m in the multipolar expansion, are given by a wakefield integral along any arbitrary contour, like (C) in Figure 1, starting and ending on the beam tubes. This integral is such that the contribution of the beam tubes vanishes. One can therefore treat more general structures by passing underneath the lowest radius material without having to introduce long beam tubes. The detailed derivation of this method is given in [2]. Its only limitation is, for $m \geq 1$, that the two beam tubes have equal radii.

This method has been implemented in the computer code ABCI [3] where the integration path is made of straight line segments defined by the 3 parameters ZCF, ZCT ans RWAK as shown in Figure 1. Results from this code are presented.

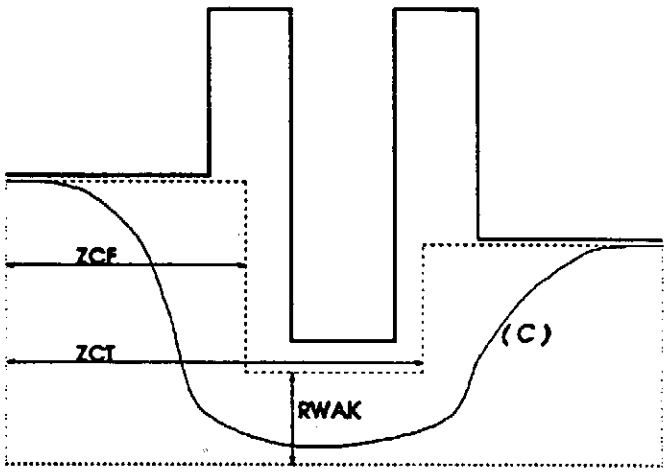

Figure 1 Contours and contour parameters in program ABCI

II. CALCULATION OF THE WAKE POTENTIALS

The longitudinal and transverse wake potentials are defined by

$$W_z(r,\theta,s) = -\frac{1}{Q}\int_{-\infty}^{+\infty} dz\, E_z(r,\theta,z,t(z,s)) \qquad (1)$$

and

$$\mathbf{W}_\perp(r,\theta,s) = \frac{1}{Q}\int_{-\infty}^{+\infty} dz\, (\mathbf{E}_\perp + \mathbf{v}\times\mathbf{B})(r,\theta,z,t(z,s)) \qquad (2)$$

where s is the distance behind the exciting charge Q of velocity v=c.

$$t(z,s) = (z+s)/c \ . \qquad (3)$$

It is convenient to decompose the electromagnetic fields as $\mathbf{E}=\mathbf{E}^{(0)}+\mathbf{E}^{(r)}$ and $\mathbf{B}=\mathbf{B}^{(0)}+\mathbf{B}^{(r)}$ where $(\mathbf{E}^{(0)},\mathbf{B}^{(0)})$ are the

fields generated by Q in free space, and $(\mathbf{E}^{(r)}, \mathbf{B}^{(r)})$ are the fields radiated by the structure and contributing to the wake potentials W_z and $\mathbf{W}_\perp$. Assuming $\theta = 0$ for the exciting charge, these fields obey the following Fourier expansion

$$(E_r, B_\theta, E_z)(r,\theta,z,t) = \sum_{m=0}^{\infty} (e_r, b_\theta, e_z)^{(m)}(r,z,t)\cos(m\theta)$$
$$(B_r, E_\theta, B_z)(r,\theta,z,t) = \sum_{m=1}^{\infty} (b_r, e_\theta, b_z)^{(m)}(r,z,t)\sin(m\theta) \tag{4}$$

Defining the 2d-vectors $\mathbf{S}^{(m)}$ and $\mathbf{D}^{(m)}$ in the *(r,z)*-plane, as

$$\mathbf{S}^{(m)} = \begin{pmatrix} r^m\left[e_r^{(r)} + cb_\theta^{(r)} - e_\theta^{(r)} + cb_r^{(r)}\right]^{(m)} \\ r^m\left[e_z^{(r)} + cb_z^{(r)}\right]^{(m)} \end{pmatrix} \tag{5}$$

$$\mathbf{D}^{(m)} = \begin{pmatrix} r^{-m}\left[e_r^{(r)} + cb_\theta^{(r)} + e_\theta^{(r)} - cb_r^{(r)}\right]^{(m)} \\ r^{-m}\left[e_z^{(r)} - cb_z^{(r)}\right]^{(m)} \end{pmatrix} \tag{6}$$

one can show, using the homogeneous Maxwell's equations satisfied by the fields $(\mathbf{E}^{(r)}, \mathbf{B}^{(r)})$, that the one-forms defined by these vectors are closed in the *(r,z)*-plane, i.e.

$$\begin{aligned} \partial_r S_z^{(m)}(r,z,s,t(z,s)) - \partial_s S_r^{(m)}(r,z,s,t(z,s)) = 0 \\ \partial_r D_z^{(m)}(r,z,s,t(z,s)) - \partial_s D_r^{(m)}(r,z,s,t(z,s)) = 0 \end{aligned} \tag{7}$$

This implies that the vectors $\mathbf{S}^{(m)}$ and $\mathbf{D}^{(m)}$ derive from a potential and that their integral along a closed contour (enclosing the vacuum) vanishes. This property allows one to deform the wakefield integration path from the straight line (L_r) at constant radius r used in definitions (1) and (2), to any contour (C).

A. The m=0 case

In this case the radiated fields $(\mathbf{E}^{(r)}, \mathbf{B}^{(r)})$ vanish at both ends of the beam tube, and the integrals of $\mathbf{S}^{(0)}$ along (L_r) and along the path (C), are equal:

$$\int_{L_r} \mathbf{S}^{(0)}(r,z,s)\cdot d\mathbf{l} = \int_C \mathbf{S}^{(0)}(r',z,s)\cdot d\mathbf{l} \tag{8}$$

The right-hand side of this equation is proportional to the longitudinal potential $W_z^{(0)}(s)$, which is therefore given by

$$W_z^{(0)}(s) = -\frac{1}{Q}\int_C \left[E_z dz + (E_r + cB_\theta)dr\right]^{(m=0)}(r,z,t(z,s)) + \frac{1}{\pi\epsilon_0}\ln\left[\frac{a_{in}}{a_{out}}\right]\delta(s) \tag{9}$$

where the log term comes from the integration of the free fields $E_r^{(0)} + cB_\theta^{(0)}$, and a_{in} and a_{out} are the tube radii.

B. The m>0 case

In that case we assume that $a_{in} = a_{out} = a$, as will be justified later. Then

$$\int_{L_r} \mathbf{S}^{(m)}(r,z,s)\cdot d\mathbf{l} = \int_C \mathbf{S}^{(m)}(r',z,s)\cdot d\mathbf{l} \tag{10}$$

$$\int_{L_r} \mathbf{D}^{(m)}(r,z,s)\cdot d\mathbf{l} = \int_C \mathbf{D}^{(m)}(r',z,s)\cdot d\mathbf{l} \tag{11}$$

since the radial integrals at $z = \pm\infty$ cancel each other. The first equation, evaluated on the z-axis, implies that the integral of $\mathbf{S}^{(m)}$ along any contour vanishes. It is then easy to show that

$$W_z^{(m)}(r,\theta,s) = -\frac{\cos(m\theta)}{2Q} r^m \int_C \mathbf{D}^{(m)}\cdot d\mathbf{l} \tag{12}$$

Adding to the integral of $\mathbf{D}^{(m)}$ the (vanishing) integral of $\mathbf{S}^{(m)}$ along (C) divided by a^{2m}, leads to an expression of the longitudinal wake potential where the integral along the beam tubes vanishes due to the metallic boundary conditions. This is however only possible when the tube radii are equal. Evaluating the resulting expression in terms of the e.m. fields in the structure, leads to

$$W_z^{(m)}(r,\theta,s) = \frac{r^m\cos(m\theta)}{2Qa^m} w^{(m)'}(s) \tag{13}$$

with

$$w^{(m)'}(s) = -\int_C dz\left[\left(\frac{a^m}{r'^m} + \frac{r'^m}{a^m}\right)e_z - \left(\frac{a^m}{r'^m} - \frac{r'^m}{a^m}\right)cb_z\right] + dr'\left[\left(\frac{a^m}{r'^m} + \frac{r'^m}{a^m}\right)(e_r + cb_\theta) + \left(\frac{a^m}{r'^m} - \frac{r'^m}{a^m}\right)(e_\theta - cb_r)\right] \tag{14}$$

The transverse potential can be written, using the Panofsky-Wenzel theorem, as

$$\mathbf{W}_\perp(r,\theta,s) = \sum_{m=1}^{\infty} \frac{mr^{m-1}}{2Qa^m}\left(\cos(m\theta)\hat{\mathbf{r}} - \sin(m\theta)\hat{\boldsymbol{\Theta}}\right)w^{(m)}(s) \tag{15}$$

with

$$w^{(m)}(s) = \frac{-1}{m}\int_C r'dr'\left[\left(\frac{a^m}{r'^m} - \frac{r'^m}{a^m}\right)e_z - \left(\frac{a^m}{r'^m} + \frac{r'^m}{a^m}\right)cb_z\right] + r'dz\left[\left(\frac{a^m}{r'^m} + \frac{r'^m}{a^m}\right)(e_\theta + cb_r) - \left(\frac{a^m}{r'^m} - \frac{r'^m}{a^m}\right)(e_r - cb_z)\right] \tag{16}$$

In equations (14) and (16), it is understood that the electromagnetic fields are projected on their multipolar component of order m, and that their argument is $(r', z, t(z,s))$.

III. COMPUTER IMPLEMENTATION

The possibility of integrating along a non-straight path, using Equations (9), (14) and (16), has been implemented in the time-domain program ABCI [3] as discussed in the introduction. We illustrate the interest of this method with the calculation of wake potentials for two cases. We first consider a 1 cm long collimator of 4 mm radius in a beam tube of 1 cm radius. Figure 2 shows a comparison of the loss factor of a Gaussian bunch with $\sigma_z = 5$ mm calculated with two different methods:

1. the wakefield integration along a straight line at 4 mm constant radius (solid line). The calculated wake potential and loss factor then depend on the length L of the tube on both sides of the collimator. The result is given, after substraction of the wake of the tube alone ("numerical noise correction" similar ot the WAKCOR method in TBCI [5]), by the asymptotic value.
2. the wakefield integration along the boundary of the collimator, using Equation (9). In this case the result is independent of the length of the tube and gives directly the value of the loss factor (dotted line).

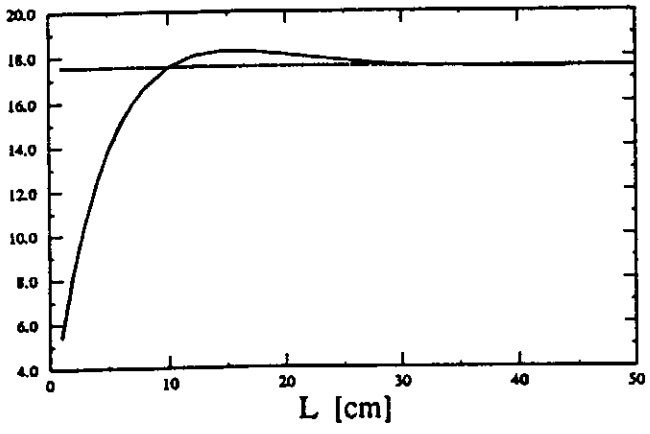

Figure 2 Longitudinal loss factor [V/pC] of a collimator as a function of the beam tube length

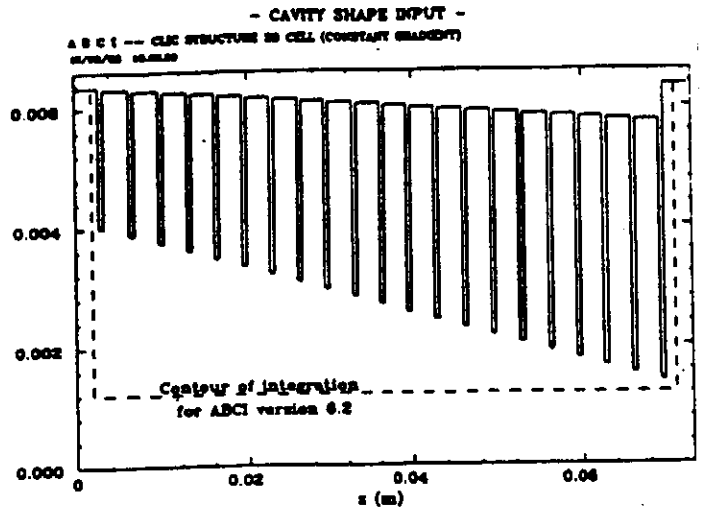

Figure 3 Constant gradient structure for CLIC

Finally Figure 4 plots the m=1 wake potentials of a 20 cell 30 GHz constant gradient structure, as shown in Figure 3, where the inner and outer radii of each cell are different. The contour of integration chosen by the program is given by the dashed line.

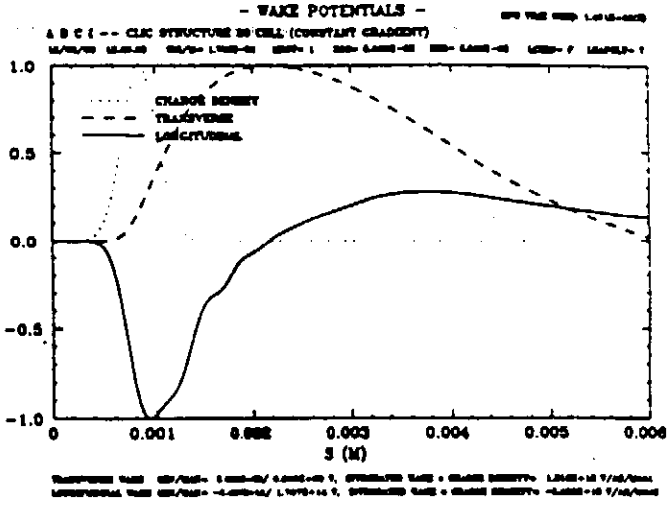

Figure 4 Dipolar wake potential (m=1)

IV. CONCLUSION

In practical calculations of the wake potentials created by axisymmetric cavities, one usually evaluates them by integrating along the cavity gap at the beam tube radius. We have generalized this method by showing that the wake potentials, of any multipole order, are given by integrals over the wake fields along any arbitrary contour spanning the structure longitudinally. By so doing we have extended the range of applications to structures of more complicated shape. The integration of wake fields along well chosen contour permits a large savings in computer capacity. In particular, the integration along a structure extending to the inside of the beam tubes - such as a collimator or iris - has become much easier with this method. Also the m=0 wake potential of structures with unequal beam tubes can be calculated in this manner. The new method of integration has been implemented in the code ABCI (versions 5 or higher) which can choose the proper contour automatically or as selected by the user.

V. REFERENCES

[1] T. Weiland, NIM 216 (1983), 31

[2] O. Napoly, Y.H. Chin, B. Zotter, DAPNIA/SEA/93-01 and CERN-SL/AP 93-14, to appear in NIM A

[3] Y.H. Chin, Report LBL-33091, CERN-SL/AP 92-49 (1992), and these proceedings

[4] W. Panofsky and W. Wenzel, Rev. Sci. Instrument, 27 967 (1956)

[5] T. Weiland, Report DESY 82-015 (1982)